ROYAL SOCIETY
OF CHEMISTRY

REVIEW

Check for updates

Absorption and polarization based on metastructures: a review

Xue-Fang He[a] and Hai-Feng Zhang ⓘ *[ab]

Metastructures (MSs) are artificial electromagnetic materials with specific design sizes, and their structure is composed of periodic or aperiodic arrangements of basic elements. These new electromagnetic materials exhibit some unique electromagnetic properties and phenomena compared with natural materials and can achieve richer and more personalized functions. Various phenomena based on MSs have attracted the interest of many researchers, among which absorption and polarization phenomena have attracted much attention due to their unique functions and properties. Different from ordinary absorbers and polarization converters (PCs), devices that are studied and designed using the absorption and polarization properties of MSs have often demonstrated better performance and unique functions and are widely used in different fields and disciplines, such as military, communications and medicine, with extensive potential. In the early days, absorbers and PCs had various problems, such as single frequency performance, poor controllability, angle sensitivity, and narrow bandwidth, and the introduction of MSs has improved and solved these problems. This article reviews the development of MS-based absorbers and PCs and describes their reconfigurable techniques, performance optimization techniques, and potential applications. In addition, it analyzes and discusses the latest research on absorption and polarization phenomena based on MSs and put forward the possible future research directions and prospects.

1. Introduction

Metastructures (MSs) are artificially engineered dielectric structures with electromagnetic properties that are not found in natural materials, and they are capable of actively regulating and manipulating electromagnetic waves (EWs). Typically composed of subwavelength unit cells, MSs can be categorized into three types based on the relationship between their structural dimensions and operational wavelength: photonic crystals, electromagnetic metasurfaces, and electromagnetic MSs. Photonic crystals[1] are artificial dielectric structures composed of a variety of media with different refractive indices that are periodically arranged, and its unit cell size is equivalent to the working wavelength. Photonic crystals selectively inhibit the propagation of specific wavelengths of light by forming a photonic band gap, similar to the control of electrons by semiconductors, thereby realizing the regulation of light waves. Electromagnetic MSs[2] are man-made materials with special

[a] College of Electronic and Optical Engineering and the College of Flexible Electronics (Future Technology), Nanjing University of Posts and Telecommunications, Nanjing, 210023, China. E-mail: hanlor@njupt.edu.cn, hanlor@163.com

[b] State Key Laboratory of Millimeter Waves, Southeast University, Nanjing, 210096, China

electromagnetic properties, which often have wavelengths much smaller than the operating wavelength, and they have some special electromagnetic properties, such as negative refraction,[3] super-transmission,[4] absorption,[5] and stealth.[6] Electromagnetic metasurfaces[7] are similar to electromagnetic MSs, but their thickness is extremely thin, and they can be regarded as two-dimensional electromagnetic MSs. Metasurfaces can achieve effective and flexible control of the propagation mode, EW phase, polarization mode, and other characteristics. The unique properties of electromagnetic MSs are not inherent characteristics of the unit materials but stem from the shape and placement of all elements in the constituent units.[8] That is, the composition, size, and arrangement of the structural units or unit cells have significant impacts on the electromagnetic properties of MSs. Therefore, precise control of the frequency, amplitude, propagation direction, polarization, and other characteristics of EWs can be achieved through rational designing.[9]

Soviet scientist Veselago[10] first proposed an important concept in 1967: the dielectric constant and magnetic permeability of left-handed materials are both negative. In addition, he successfully predicted unique electromagnetic phenomena, such as negative refraction, inverse Doppler frequency shift, inverse Doppler effect, and anomalous Cerenkov radiation, in left-handed materials. Owing to the lack of left-handed

materials in nature, these advanced theories were not valued and developed for a considerable period of time. In 1996, a turning point occurred when Pendry et al.[11] first verified the existence of a negative dielectric constant using thin metal wire structures arranged periodically in a cubic lattice. Then, in 1999, it was demonstrated that the effective magnetic permeability obtained by using split rings can be adjusted to values that cannot be obtained in natural materials. The experiments of Pendry and other scholars confirmed Veselago's theory on negative dielectric constant and magnetic permeability and further promoted the development of electromagnetic MSs. Based on Pendry's research work, Professor Smith[12] successfully measured the negative refractive index of copper composite materials in 2001 and prepared the world's first electromagnetic MS. The results were published in the journal Science, sparking enthusiasm for the study of MSs. In 2006, Pendry et al.[13] conducted further research and proposed the theory of transformation optics, which means that arbitrary control of EWs can be achieved through the design of MSs.[14] They also provided design ideas and implementation schemes, further promoting the research on MSs that can freely control electromagnetic parameters.

With the advancements in research, regulatory devices designed based on MSs continue to emerge, such as invisibility cloaks,[15–18] sensors,[19–21] perfect absorbers,[22–25] polarization converters[26–29] and radar antennas.[30–32] These devices have been widely used in fields such as national defence and security, aerospace, communication technology, and other emerging technologies. Among various MS devices, absorbers and polarization converters (PCs) are widely used in various fields and play an indelible role.

The main structure of an absorber usually includes a resonant unit and a dielectric substrate. The absorption of incident EWs by absorbers is converted into other energy by matching impedance.[33] The polarization of EWs refers to the variation of the electric field strength vector over time. If the variation follows a certain pattern, they are called polarized EWs. These can be divided into three types, namely linear polarization, circular polarization, and elliptical polarization. The endpoint trajectories of their electric field intensity vector correspond to straight line segments, circles, and ellipses, respectively.[47–49] In MSs, absorption and polarization are mutually influential, and the impact of polarization on the absorption of MSs depends on their anisotropy or isotropy. When electromagnetic waves strike an MS, impedance matching causes these waves to be converted into thermal energy through ohmic, dielectric, and magnetic losses. In isotropic MSs, the absorption of linearly, circularly, and elliptically polarized waves remains consistent before and after polarization, meaning the absorption characteristics stay unchanged. However, when the MS exhibits anisotropy, the matching impedance varies with different polarization states, thereby affecting absorption. This demonstrates that polarization influences the absorption properties of MSs. Since most MSs are anisotropic, polarization is generally recognized as a significant factor affecting their absorption performance.

The absorption of MSs is primarily influenced by the symmetry of their structural units. For linearly polarized waves, the absorption efficiency is highly dependent on the relative angle between the polarization direction and the hyperstructure configuration, demonstrating polarization sensitivity. However, highly symmetric structures exhibit a small absorption difference under linear polarization, even achieving polarization insensitivity at large angles. For circularly polarized waves, the absorption performance depends on chirality. Chiral structures show significant absorption differences between left-handed and right-handed polarizations, whereas symmetric structures demonstrate identical absorption for vertically incident left-handed/right-handed circular polarizations, without noticeable effects. As the most general form, elliptically polarized waves are typically considered the superposition of two distinct circular polarizations with different chirality directions. Consequently, the absorption performance of these hyperstructures is influenced by both ellipticity and the orientation angle.

Early absorbers had high absorption rates (ARs) for a specific frequency, limited absorption bandwidth, poor tunability, polarization sensitivity, and other issues, which restricted their applications. The advantages of MSs lie in their unique electromagnetic properties that enable the precise control of incident electromagnetic waves. Compared with other traditional materials, they can better regulate the operating frequency and bandwidth, while achieving higher absorption rates and polarization conversion efficiency (PCR). Additionally, with the use of tailored materials and active devices during design, MSs can switch between operating frequency bands and states. This means that MSs possess advantages, such as compact size, easy integration, diversified functions, high performance, strong personalization, and excellent tunability. Therefore, absorbers based on MSs have the advantages such as low thickness, stronger absorption effect, light weight, and the ability to dynamically control electromagnetic parameters. In both military and civilian fields, their application potential is enormous, including in radar stealth,[34,35] thermal radiation stealth,[36,37] electromagnetic shielding,[38,39] wireless energy transmission[40,41] and other fields, providing important technical support to meet the rapid development needs of modern information technology.[42] By introducing MSs and researching the design technology, device performance has been greatly improved, and its functionality has been greatly expanded. For example, the frequency domain of electromagnetic MS absorbers has expanded from the microwave band and gigahertz (GHz) to terahertz (THz),[43] near-infrared,[44] far-infrared,[45] and visible light bands.[46]

In practical applications, it is often necessary to detect or change the polarization characteristics of EWs, such as the conversion of linearly polarized waves into circularly polarized waves, which play an important role in antenna design, optical communication, polarization filters, and other fields.[50] An MS-based PC is a device that utilizes MS to achieve the polarization state conversion of EWs. Through its unique structure and material properties, it can effectively achieve this. This type of converter is typically composed of multiple layers of metal or dielectric topological structures, with a simple design and easy integration. Compared with conventional devices, PCs based on MSs have a lot of advantages, including simple design, small

This journal is © the Owner Societies 2025

Phys. Chem. Chem. Phys., 2025, **27**, 25720–25742 | **25721**

size, thinness, easy integration, flexible design, and customizable electromagnetic parameters.[51] They have broad application prospects in fields such as antennas,[52–55] sensing,[56–58] radar[59,60] and imaging.[61,62]

Studying the design technology of MS-based PCs can help improve the efficiency of PC design and enhance its flexibility, controllability, and ability to control EWs. However, their sub-wavelength dimensions and complex structural models pose challenges in their manufacturing processes, leading to higher costs. Moreover, the absorption and polarization effects of MSs are closely related to their structural models, resulting in significant variations in performance under different incident angles. This sensitivity to incident angles and polarization makes them prone to polarization sensitivity issues. Therefore, MSs also have problems, such as incident angle sensitivity, polarization sensitivity and bandwidth limit.

In this work, as illustrated in Fig. 1, we present the design and investigation of absorption and polarization functions based on MSs from four key perspectives: historical review, design techniques, recent research advances, and challenges and prospects. The organization of this article is outlined in Fig. 2. We begin by defining and categorizing the concept of MSs, followed by a review of the development history of MS-based absorbers and polarization converters (PCs). We then provide a detailed introduction to the design methodologies used for these devices, covering both reconfigurable technologies and performance enhancement strategies, along with examples of specific applications. The subsequent sections explore recent research and application trends in MS-based absorption and polarization control. Finally, the article concludes with a summary of findings and a discussion on the current challenges and future prospects in the field.

2. Development of absorbers based on MSs

The development of MS-based absorbers can be traced back to 2008, when Landy *et al.*[23] first proposed an absorber design based on an MS and experimentally verified its functionality.
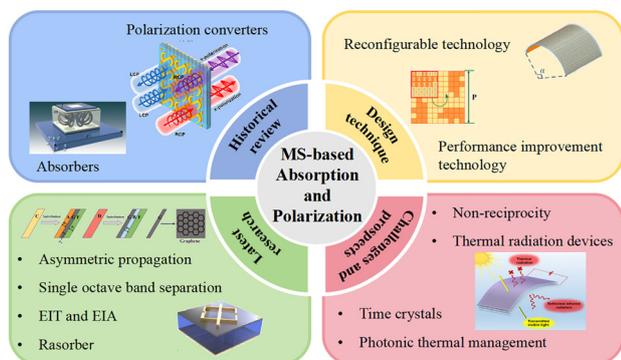

Fig. 1 . Summary of the review: absorption and polarization based on MSs from four aspects, namely, historical review, design techniques, latest research, and challenges and prospects.
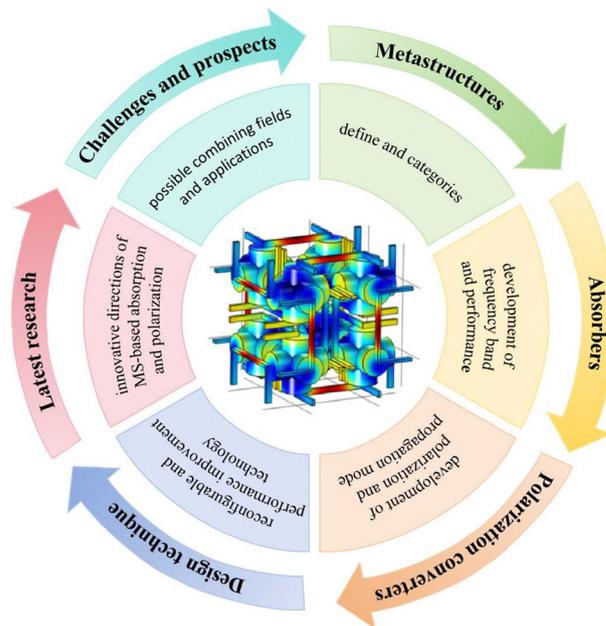

Fig. 2 Roadmap of the review, showing the progression of topics.

As shown in Fig. 3(a), the absorber was composed of a square electric resonator, a dielectric substrate, and short wires from the top to bottom, achieving nearly 100% absorption at 11.65 GHz and high absorption near a narrowband. This research pioneered the use of MS in designing light absorbers. Compared with traditional absorbers,[63] these have higher ARs, smaller sizes, thinner and lighter masses, along with richer potential applications. However, this type of absorber only has high AR at specific frequencies, which limits its application. In contrast, broadband MS-based absorbers have a wider absorption frequency range, stronger adaptability, and better electromagnetic compatibility, which make them more widely applicable. Since 2010, the absorption frequency range of MS-based absorbers has gradually expanded from single-frequency points[64,65] and multi-frequency points[66,67] to broadband.[68,69] In 2010, Li *et al.*[70] designed a dual-band MS absorber consisting of four resonators rotated at 90°, as shown in Fig. 3(b). The simulation results demonstrated that this absorber had two perfect absorption points near 11.15 GHz and 16.01 GHz, which respectively maintained ARs of over 90% and 92%. In 2018, Shrestha *et al.*[71] proposed a broadband infrared metasurface absorber using indium tin oxide and an asymmetric Fabry Perot cavity, as shown in Fig. 3(c). In the 4–16 μm wavelength range, its AR exceeded 80% and remained stable over a wide range of incident angles. In 2020, Fan *et al.*[72] designed a broadband electromagnetic MS absorber loaded with patch resistors, as shown in Fig. 3(d). This design exhibited an AR of over 90% and a relative bandwidth (RB) of over 119.2% in the frequency range of 2.55–10.70 GHz. Compared with other absorbers, loading surface-mount resistors in metal resonant structures has two main advantages. On the one hand, it can effectively adjust the equivalent impedance and achieve maximum AR by achieving a perfect impedance matching; on the

25722 | *Phys. Chem. Chem. Phys.*, 2025, **27**, 25720–25742
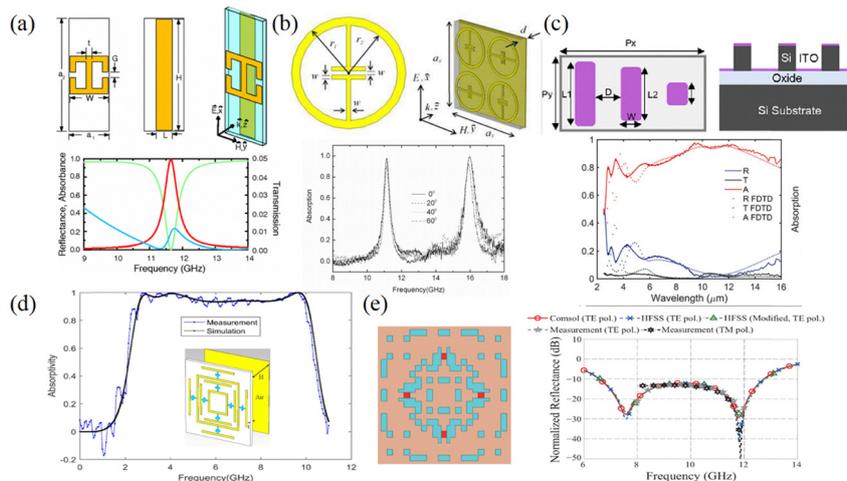
This journal is © the Owner Societies 2025

Fig. 3   (a) First MS-based absorber. Reproduced from ref. 23 with permission from Physical Review Letters, copyright 2008. (b) Dual-band MS absorber. Reproduced from ref. 70 with permission from Progress In Electromagnetics Research, copyright 2010. (c) Broadband infrared MS absorber. Reproduced from ref. 71 with permission from Acs Photonics, copyright 2018. (d) Broadband MS absorber loaded with patch resistors. Reproduced from ref. 72 with permission from Materials, copyright 2020. (e) Broadband MS absorber composed of square copper tiles. Reproduced from ref. 73 with permission from Materials, copyright 2023.

other hand, surface mount resistors can convert surface current into heat for consumption and have a good absorption effect on incident EWs. In 2023, Kim *et al.*[73] reported a broadband MS absorber consisting of square copper tiles connected to four chip resistors, as shown in Fig. 3(e). According to the computed results, it had a wide RB of −10 dB and a fractional bandwidth of 63.83% from 6.57 to 12.73 GHz. It is worth mentioning that in this work, the optimal combination of copper tiles was obtained by applying a genetic algorithm (GA) for automatic program design to achieve broadband absorption. The use of a genetic algorithm greatly improved the design efficiency and optimized system performance. The above-mentioned studies on electromagnetic MS

absorbers provide different methods and design ideas for achieving broadband design goals, making important contributions to the construction of frequency-diverse communication systems and advancing the field of MS-based absorbers.

In addition, the operating frequency domain of MS-based absorbers has gradually expanded from the microwave band[74,75] to THz,[76,77] near-infrared,[78,79] far-infrared,[80,81] and even visible light band.[82,83] In 2008, the team of H. Tao at the University of Central Florida in the USA[24] extended the MS-based absorbers to the THz band-based on the "double opening split ring resonators (SRRs) dielectric layer metal wire" structure for the first time, as shown in Fig. 4(a), with an AR of 70% at
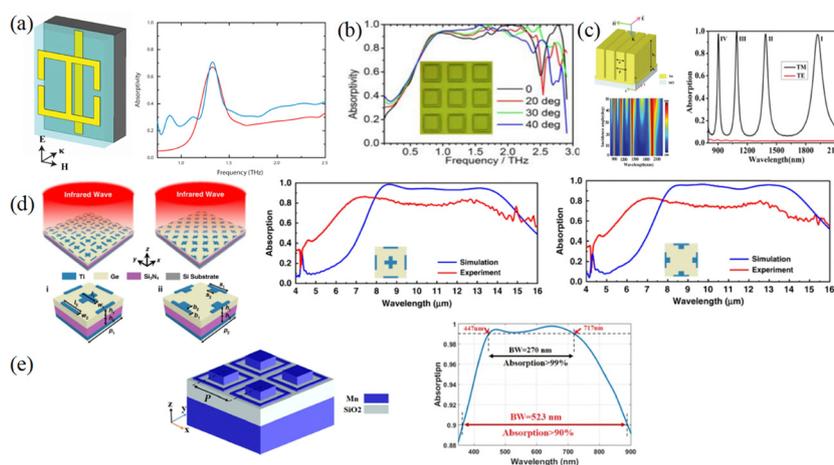

Fig. 4   (a) Absorber with a "dual opening SRRs dielectric layer metal wire" structure. Reproduced from ref. 24 with permission from Optics Express, copyright 2008. (b) Broadband absorber made of a metal dielectric multilayer composite material. Reproduced from ref. 84 with permission from Applied Physics Letters, copyright 2014. (c) Multi-frequency absorber in the near-infrared band, with a metal grating structure. Reproduced from ref. 85 with permission from IEEE Access, copyright 2020. (d) Perfect absorber in the long-wavelength infrared range. Reproduced from ref. 81 with permission from Light: Science & Applications, copyright 2021. (e) Broadband absorber with a manganese−silicon dioxide−manganese three-layer structure. Reproduced from ref. 86 with permission from Scientific Reports, copyright 2023.

1.3 THz. Although the absorption efficiency reported in this work was not very high and offered a single-frequency point absorption, this work made a pioneering contribution to identifying applications in the THz band, providing ideas for subsequent research and design. In 2014, Zhu *et al.*[84] prepared an ultra-wideband absorber in the THz frequency domain using metal dielectric multilayer composite materials, as shown in Fig. 4(b), with an AR of over 80% in the 0.7–2.3 THz range. The RB of this design was about 127%, which was bigger than the total absorption width of the THz frequency previously reported and indicated higher practicality. In 2020, Wu *et al.*[85] presented a multi-frequency MS absorber based on a metal grating structure that could operate in the near-infrared band, as shown in Fig. 4(c). The results indicated that for transverse magnetic (TM) wave incidence, the absorber presented four different absorption peaks, with an AR exceeding 97%. For transverse electric (TE) wave incidence, the AR approached zero in the operating frequency domain. In 2021, Zhou *et al.*[81] designed a perfect absorber with an ultra-wideband in the long-wave infrared range. As shown in Fig. 4(d), both types of Ti/Ge/Si$_3$N$_4$/Ti absorbers exhibited high ARs exceeding 90% over a wide wavelength range from 8 to 14 μm, covering the entire long-wave infrared range. This absorber can exhibit perfect broadband absorption in the ultra-long infrared wave range and has the advantages of small size, simplicity, and low cost. It may be applied in fields, such as thermal emitters, infrared imaging, and photo detectors in the future. In 2023, Sayed *et al.*[86] proposed a broadband absorber with a manganese–silicon dioxide–manganese three-layer structure and optimized various parameters using the particle swarm optimization algorithm (PSO). As shown in Fig. 4(e), the optimal parameters can achieve absorption of over 94% in the visible-light range, with an average AR of 98.72%, and even a perfect AR of over 99% in the 447–717 nm range. At present, the application of MS-based absorbers has significantly expanded to various frequency domains, not only expanding the application scope of the absorbers, but also meeting the growing demand for high-frequency applications.

Traditional absorbers often exhibit instability when facing EWs with large angles of incidence or different polarization states, which limits their application in complex electromagnetic environments. Therefore, improving the angle and polarization insensitivity of absorbers is one of the significant directions in current research, and there have been many solutions so far. In 2010, Zhu *et al.*[87] proposed a polarization-insensitive microwave absorber by using an MS, as shown in Fig. 5(a). Its lattice unit consisted of a quadruple, rotationally symmetric electric resonator and a cross structure at the bottom of the dielectric substrate to achieve electrical and magnetic resonance, effectively absorbing the incident wave energy. For incident EWs of different polarizations, the microwave AR was 97%, and the absorption efficiency of TE and TM waves reached over 90% in a wide incident angle range of 0° to 60°. In 2018, Nguyen *et al.*[88] designed a broadband MS absorber consisting of eight resistance-arm units, as shown in Fig. 5(b), which was suitable for X-band (8.20–12.40 GHz) applications and achieved broadband and wide-angle absorption. From 8.20 to
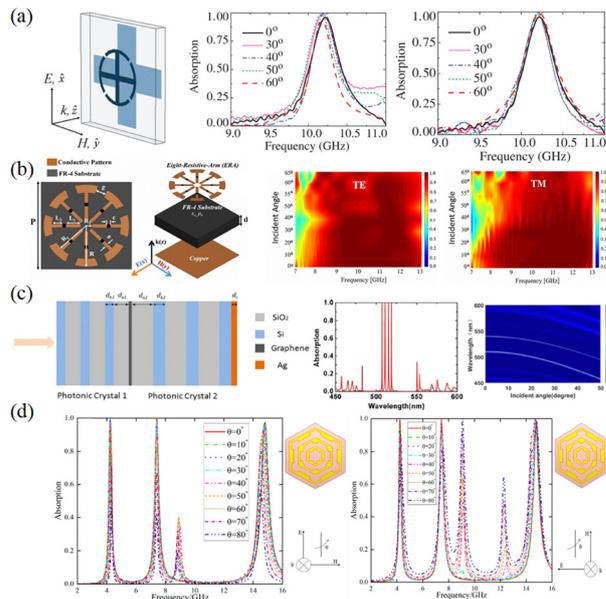

Fig. 5 (a) Polarization-insensitive microwave absorber based on an MS. Reproduced from ref. 87 with permission from Progress In Electromagnetics Research, copyright 2010. (b) Broadband MS absorber composed of eight resistance-arm units. Reproduced from ref. 88 with permission from Scientific Reports, copyright 2018. (c) Multi-channel absorber with one-dimensional graphene topological photonic crystals. Reproduced from ref. 89 with permission from Optics Letters, copyright 2018. (d) Ultra-thin incident-angle-insensitive three-band absorber. Reproduced from ref. 91 with permission from MDPI, copyright 2025.

13.40 GHz, the AR of the MS absorber was greater than 90% at any polarization angle. In both TE and TM modes, the EWs maintained high ARs when the incident angle was increased from 0° to 60° and 65°. In the same year, Wang *et al.*[89] presented a multi-channel absorber made of graphene one-dimensional topological photonic crystals, as shown in Fig. 5(c). The results showed that the multi-channel absorption peaks of the perfect absorber were very narrow, and the AR exceeded 97% at incident angles of 0° to 50°. In 2021, Jiang *et al.* proposed a novel optical microwave absorber[90] that used square spiral elements in the impedance layer to increase the absorption bandwidth and improve stability under high angles of incidence. The experimental results showed that by using planar and conformal configurations with different curvatures, the absorber achieved a transmittance of 69.4%, a wide absorption band of 85.7%, excellent angular stability at 60°, and polarization insensitivity at various angles. In 2025, Zheng *et al.*[91] proposed an ultra-thin three-band MS absorber, with an incident-angle-insensitive structure consisting only of metal patches, dielectric layers, and copper grounding, as shown in Fig. 5(d). This absorber showed a high AR and three absorption bands, covering the C-band, X-band, and K-band. As mentioned above, by designing new structures (such as quadruple rotationally symmetric resonators, cross structures, and square spiral elements) and optimizing the material parameters (such as the introduction of impedance layers and compensation layers), the stable absorption ability of the absorbers to various incident angles and

polarization states of EWs can be improved to meet the needs of radar systems and communication equipment. The excellent angle stability performance makes these devices widely applicable in multiple fields, as they can effectively absorb EWs in various complex environments, reduce electromagnetic interference, protect sensitive equipment, and promote the overall operation of the system.[42]

A review of the research progress in the operating frequency band and performance of MS-based absorbers reveals that by adopting different design schemes, this type of absorber has successfully achieved broadband design goals, and its application frequency band has also extended to the THz, near-infrared, far-infrared, and even visible light bands. More importantly, the existing MS absorbers exhibit excellent angular stability at different incident and polarization angles, achieving efficient absorption of EWs over a wide range of incident and polarization angles. However, the research on traditional absorbers in various frequency bands has become relatively saturated, and the electromagnetic environment in practical scenarios has become more complex and varied. Traditional single-function absorbers can no longer meet the growing scientific and application needs. Therefore, developing absorbers with multifunctionality and tunability is a new challenge yet necessary for addressing future electromagnetic environments.

3. Development of PCs based on MSs

In 2007, Hao et al.[92] proposed the theory that the polarization state of EWs can be effectively controlled using anisotropic materials, and by adjusting material parameters, various possible polarization modes can be achieved. They also designed an "I-shaped" pattern of an MS-based PC, as shown in Fig. 6(a) for verification. Through microwave experiments, it was verified that the PC could completely convert linearly polarized EWs into cross-polarized EWs. The PC achieved a polarization conversion rate of over 90% at 6.80 and 12.86 GHz. This work successfully demonstrated the possibility of applying MSs to manipulate the polarization state of EWs, providing a direction for future research. Subsequently, PCs based on MSs gradually emerged for conversion between various polarization states. In 2018, Xu et al.[93] designed an H-shaped line-to-line PC based on an MS, as shown in Fig. 6(b). In the frequency range of 7.00–19.50 GHz, this polarization converter could achieve over 90% PCR and an RB of 94%. This PC met the ultra-wideband requirements and had a simple surface structure that was easy to process. In 2019, Guo et al.[94] used a photonic crystal plate structure to achieve arbitrary linear polarization conversion, as shown in Fig. 6(c). Even when the incident light direction was changed, for a fixed input polarized light, reflected light with any output polarization could be generated. In 2024, Hafeez et al.[95] designed a multi-band and multifunctional metasurface, which achieved linear and circular polarization conversion in the reflection mode. As shown in Fig. 6(d), the PCR reached over 95% in specific bands. From the above
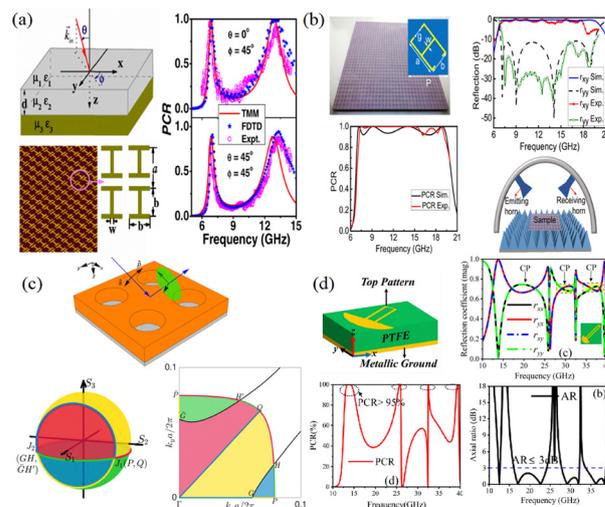

Fig. 6 (a) MS PC with an I-shaped structure. Reproduced from ref. 92 with permission from Physical Review Letters, copyright 2007. (b) H-shaped linear MS PC. Reproduced from ref. 93 with permission from Optics Express, copyright 2018. (c) Arbitrary linear polarization converter based on a photonic crystal plate structure. Reproduced from ref. 94 with permission from Advanced Optical Materials, copyright 2019. (d) Multi-band linear circular polarization conversion metasurface. Reproduced from ref. 95 with permission from Crystals, copyright 2024.

studies, it can be seen that PCs based on MSs overcome the shortcomings of narrow bandwidth and low conversion rates observed in the past. Their working band is wider, and the polarization conversion function is improved and no longer limited to one-way conversion, making them better suited for imaging, remote sensing, and satellite communication systems.

PCs often need to work in conjunction with radiation sources to achieve polarization conversion of EWs. Based on the positional relationship between the radiation source and the converted EWs, they can be divided into reflective[96–98] and transmissive[99–101] MS PCs. Below given are two types of PCs, provided for example introduction and analysis comparison.

In 2015, Gao et al.[102] proposed a dual V-shaped reflective MS PC. Computed results showed that in the ultra-wideband range of 12.40–27.96 GHz, the PC can effectively convert linear polarization into cross polarization, with an average PCR of 90%. This PC has a simple structure but can achieve ultra-wideband effects, suitable for various application scenarios, and can be extended to the THz band. In 2021, Guo et al.[103] presented a linear PC based on an MS that operates in the reflection mode, as shown in Fig. 7(a). In the frequency range of 4.73–10.93 GHz, the PCR of the PC exceeded 90%. The converter showed angular stability below 36° and superior polarization insensitivity under x- and y-polarized incident waves.

In 2018, Lin et al. proposed a broadband transmission linear-to-circular conversion PC based on metasurfaces.[104] The converter consisted of three conductive pattern layers, each containing a square array of elliptical ring apertures. As shown in Fig. 7(b), this PC achieved linear-to-circular polarization conversion, with a relative bandwidth of 40.2% within the
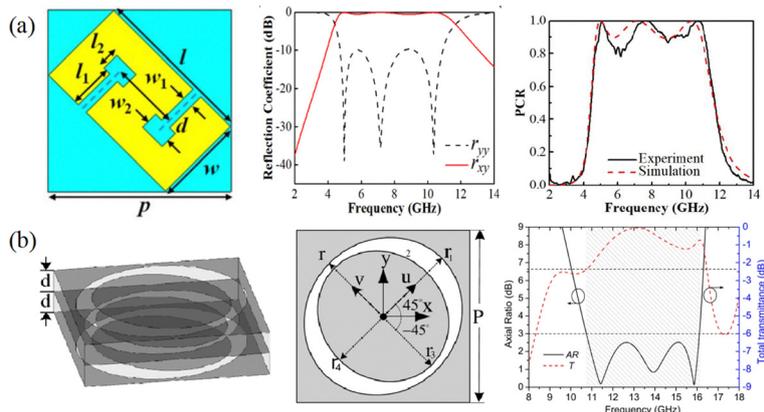
Fig. 7 . (a) Reflective PC based on MSs. Reproduced from ref. 103 with permission from Engineered Science, copyright 2021. (b) Broadband transmission linear-to-circular conversion PC based on metasurfaces. Reproduced from ref. 104 with permission from Applied Physics A, copyright 2018.

10.73–16.13 GHz frequency range. In 2022, Chandra et al.[101] designed an ultra-thin transmissive MS cross PC that achieved the conversion of linearly polarized waves to cross-polarized waves in the C, X, and Ku frequency bands, and the PCR exceeded 95% at frequencies from 4.6 to 14.8 GHz.

In general, various PCs have been designed and manufactured to effectively meet the needs of today's antenna systems, communication systems, and coding imaging fields. PCs based on MSs exhibit distinct characteristics and advantages in different polarization modes and propagation modes, but there are also some shortcomings. For instance, reflective converters may introduce additional reflections and scattering, causing interference to communication systems. However, the transmission PC may be limited by the transmission performance of the material, which affects the efficiency of polarization conversion. To effectively address the limitations of different types of PCs and improve device performance, traditional MS-based PCs are gradually being integrated with tunable materials, shifting towards the development of multifunctional electromagnetic intelligent devices.

4. Design techniques and methods

By reviewing the development history of MS-based absorbers and PCs, we can understand that their functions have made significant breakthroughs, and their performance has been greatly improved. We have also discovered the important contributions of various MS design technologies in addressing developmental bottlenecks and limitations. This section summarizes the commonly used effective design techniques, with a focus on the application of reconfigurable technology and performance improvement technology in absorbers and PCs. Among them, reconfigurable technology refers to the flexible adjustment of the electromagnetic properties of MSs, while performance improvement technology focuses on enhancing the electromagnetic properties and functional performance of MSs. By optimizing the material structure, size, resonance mechanism, and other aspects of MSs, their performance can be significantly improved, and their application scope

can be expanded to meet the growing demands of different applications.

4.1. Reconfigurable technology

Reconfigurable technology is the controllable adjustment of the performance or electromagnetic response of MSs using external stimuli or internal control measures. This technology can change the electromagnetic properties of MSs, enabling flexible and efficient electromagnetic control in different working environments or application scenarios. As shown in Fig. 8, three reconfigurable technologies that can be applied to absorbers and PCs are the use of tailored materials[105,106] (graphene, vanadium dioxide (VO$_2$), liquid crystal and photosensitive materials), active devices[69,107] (PIN diodes, varactor diodes and solid-state plasma) and gravity fields.

Tunable materials can switch their states under external excitation, including electrical, magnetic, laser, pressure, temperature, and chemical factors. By changing the geometric or physical parameters of the resonators of the MS, discontinuous
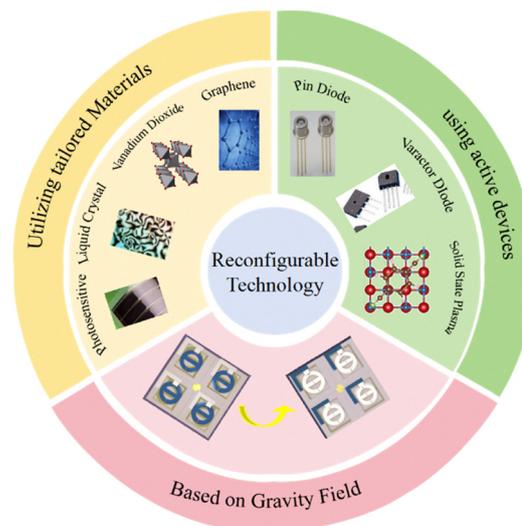

Fig. 8 Classification of reconfigurable technologies.

25726 | *Phys. Chem. Chem. Phys.*, 2025, **27**, 25720–25742

This journal is © the Owner Societies 2025

phases at the exit interface can be obtained, thereby designing dynamically controlled multifunctional MSs. It offers diverse regulatory characteristics and flexible modulation methods and is widely used in the reconfigurable design of MSs. It is also an important and common reconfigurable method used for absorbers and PCs based on the MS.

In 2007, physicists K. S. Novoselov and A. K. Geim of the University of Manchester, UK, successfully prepared a single-layer graphene[108] using a mechanical stripping method. This is a two-dimensional plane material, which consists of a hexagonal lattice of closely arranged single-layer carbon atoms, with the characteristics of a semi metal with no gap. Graphene has excellent photovoltaic properties,[109–111] including excellent light transmittance, ultra-wide response spectrum, and fast photovoltaic response, making it important for applications in cutting-edge fields, such as detection and optoelectronic sensing. Furthermore, the conductivity of graphene can be flexibly adjusted through bias voltage,[112] and thus it demonstrates excellent potential in tuning MSs and can be well applied in the design of MS absorbers and PCs. For instance, in 2018, Liu *et al.*[113] proposed graphene-based broadband metamaterial absorbers whose absorption bandwidth and efficiency could be voltage-controlled, as shown in Fig. 9(a). The results demonstrated that the single-ring absorber achieved a bandwidth of 2.25 THz across a 90% absorption range. Furthermore, they proposed combining two or more resonant rings of different sizes within a single unit cell to attain broadband absorption, with a bandwidth of 3.2 THz and higher absorption efficiency. In addition, in 2021, Zhang *et al.*[114] proposed a tunable THz PC based on cross-shaped graphene patches and their complementary structures, as shown in Fig. 9(b). By utilizing the cross graphene-patch structure, the PCR achieved over 90% cross polarization conversion from 2.92 to 6.26 THz; while utilizing its complementary structure, linear circular polarization conversion was achieved from 4.45 to 6.47 THz.

VO_2 is a compound with multiple phase transition characteristics and exhibits different crystal phases at different temperatures and pressures, with the most significant being the transition from monoclinic to orthorhombic crystal phases.[115–117] When the temperature is below 68 °C, it exhibits a monoclinic crystal phase and an insulating or semiconducting state; When the temperature exceeds 68 °C, its structure transforms into the orthorhombic crystal phase, and it changes to a metallic state. The phase transition temperature of VO_2 is low; it is easy to control, and has chemical stability and a high temperature coefficient of resistance at room temperature.[118] Most importantly, the phase transition process of VO_2 is reversible and can be well applied in the design of tunable MS devices, achieving switching between absorption and polarization conversion functions. For instance, Yan *et al.*[119] proposed a multifunctional MS through VO_2 phase transition
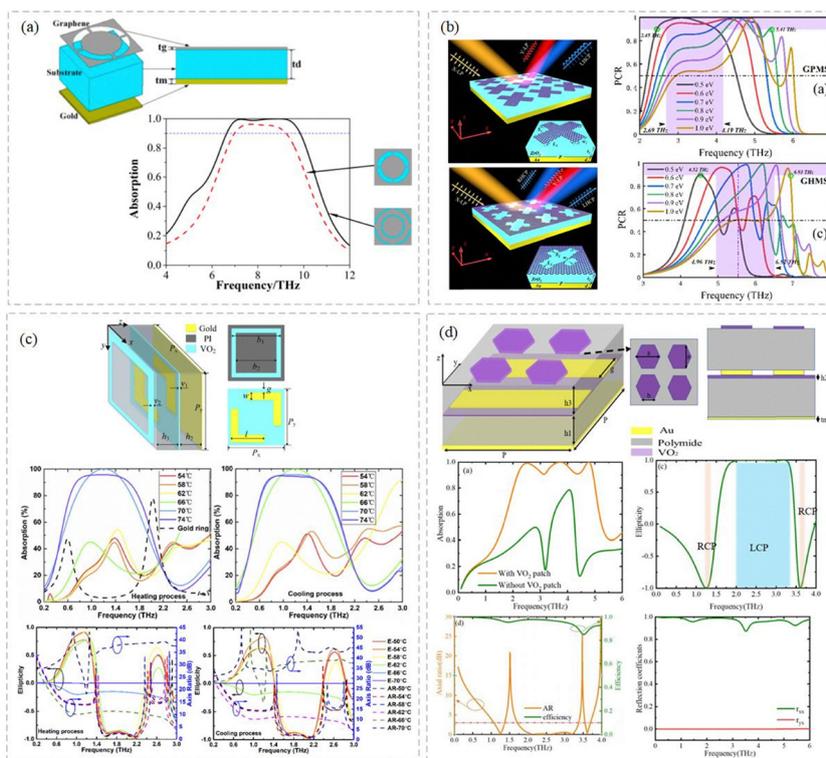

Fig. 9 (a) Graphene-based broadband metamaterial absorbers. Reproduced from ref. 113 with permission from AIP Advances, copyright 2018. (b) Single-layer tunable THz PC with a cross-shaped graphene patch and its complementary structure. Reproduced from ref. 114 with permission from Optics Express, copyright 2021. (c) Multi-functional MS based on VO_2. Reproduced from ref. 119 with permission from Optics Express, copyright 2020. (d) MS based on VO_2. Reproduced from ref. 120 with permission from Optics Express, copyright 2020.

This journal is © the Owner Societies 2025

Phys. Chem. Chem. Phys., 2025, **27**, 25720–25742 | **25727**

in 2020, as shown in Fig. 9(c). The results demonstrated that it achieved over 90% broadband absorption at 0.74–1.62 THz and broadband line circular polarization conversion function at 1.47–2.27 THz. In 2022, Qiu et al.[120] proposed an MS based on a VO₂ phase transition, as shown in Fig. 9(d), which displayed functions, such as broadband absorption, cross polarization conversion, line-to-circular polarization conversion, and total reflection in different frequency bandwidths.

In addition, liquid crystal materials and photosensitive materials can also be applied in the reconfigurable design of MS absorbers and PCs. Liquid crystal is a widely used anisotropic material, and its dielectric constant tensor can be continuously adjusted by using a bias voltage,[121] making it a candidate for tunable materials. It has many advantages, such as low cost, wide operating frequency band, weak demand for external bias voltage due to the influence of external electric and magnetic fields, and easy implementation. In 2017, Wang et al.[122] proposed a tri-frequency tunable THz MS absorber based on liquid crystals. As shown in Fig. 10(a), during the entire tuning process, the absorbance of each peak in the three frequency bands remained above 99%. In 2021, Sanusi et al.[123] proposed a multifunctional reconfigurable MS by using liquid metal injection, which could flexibly switch between four states. This MS consisted of two switchable microfluidic layers, which served as reflectors with empty channels, and the state of the liquid filled in different layers corresponded to different functions. At 9.83–17.42 GHz, it achieved linear-to-cross polarization conversion, with a PCR exceeding 90%. In addition, the MS could switch linear to circular PC at 8.97–11.30 GHz (RB = 23%). Photosensitive semiconductors are materials that can regulate conductivity through external pump illumination, such as photosensitive silicon, germanium, and gallium arsenide. They are commonly used in optical switches and have been widely applied in MS absorbers and PCs. In 2020, Li et al.[124] proposed a frequency switchable MS absorber using photosensitive germanium and gallium arsenide as optical switches embedded in a raised square ring resonator. Because photosensitive silicon and germanium can be excited using pump lights of different wavelengths, their switching states could be independently controlled. When photosensitive silicon and germanium were in different states, they could achieve single-frequency absorption at low and high frequencies and dual-frequency absorption modes. In 2022, Liao et al.[125] presented a THz MS based on the optical waveguide effect, as shown in Fig. 10(b), which achieved polarization conversion and absorption function switching. By exposing silicon to light of different intensities to achieve photoconductivity, switching between different functions was achieved. When the device was operated as a PC, it achieved conversion between linear polarization at 0.96–1.47 THz, with a PCR exceeding 90% and an RB of 42%. When silicon was excited using pump light, the device switched to an ultra-wideband absorber, with a high AR of over 90% at 0.75–1.73 THz and an RB of 79%.

Besides, the use of active devices is also an important way of designing tunable MS absorbers and PCs. Commonly used active devices[126] include PIN diodes,[127,128] varactor diodes,[129,130]
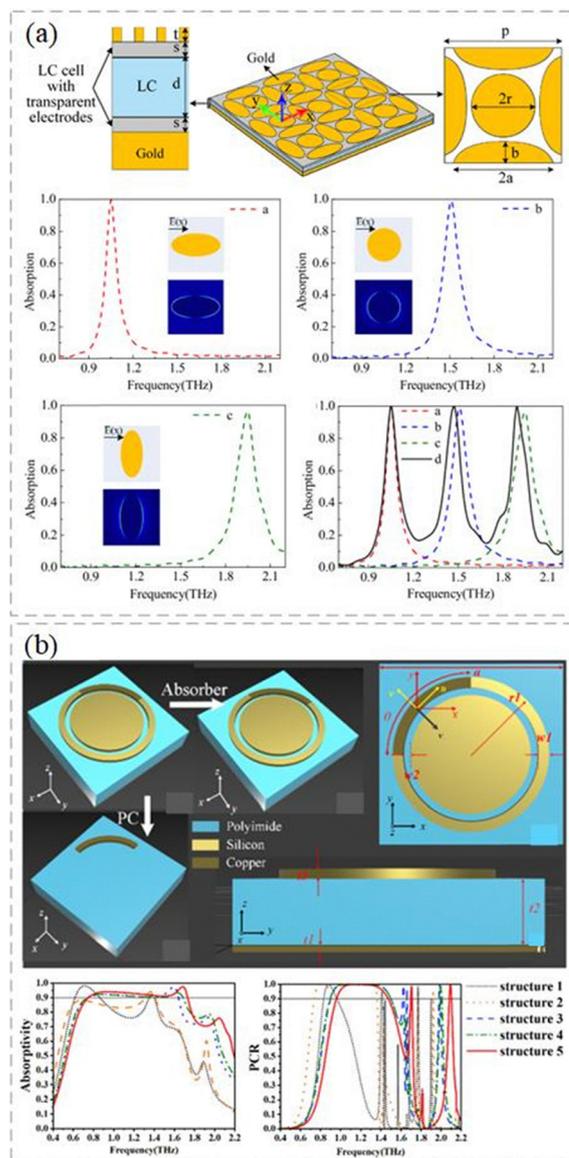

Fig. 10 (a) Three-frequency-tunable perfect THz MS absorber based on liquid crystals. Reproduced from ref. 122 with permission from Optics Express, copyright 2017. (b) Electromagnetic MS based on optical conductivity. Reproduced from ref. 125 with permission from Optics Express, copyright 2022.

and solid-state plasma,[131,132] which typically have a short response time, small sizes, and low cost. In 2018, Phon et al.[133] designed and implemented a novel multifunctional reconfigurable active electromagnetic MS. Four transmission states were achieved by controlling the bias states of the top and bottom PIN diodes separately, including reflection, transmission, and absorption. The solid-state plasma effect is a collective effect generated by charged carriers in solids.[131] When the concentration of free charges in the solid-state plasma unit is low, it is in an unexcited state and exhibits a dielectric-like state. When the concentration increases to a certain value, the unit can exhibit metal-like properties. By selectively exciting units at different positions with controllable voltage, the resonator

25728 | Phys. Chem. Chem. Phys., 2025, **27**, 25720–25742

This journal is © the Owner Societies 2025

structure and material properties can be changed to achieve device reconfigurability. In 2020, Li et al.[132] proposed a multi-functional PC that could be tuned in terms of both function and frequency. By changing the solid-state plasma excitation region to form unit patterns of different shapes, cross-polarization conversion and line circular polarization conversion functions were realized, and the transition between different operating frequency bands was realized in the cross-polarization conversion state. Reconfigurable technology based on active devices not only provides high flexibility and tunability, but also faces challenges, such as complex feed structure design, power consumption, and heat dissipation.

Compared with traditional tunable polarization-controlled MS, designing tunable MSs using gravity fields has the advantages of simple and convenient control methods, and no side effects. At present, this reconfigurable technology has become increasingly mature and has achieved some outstanding results in the applications of MS absorbers and PCs. In 2019, Tian et al.[134] proposed an innovative idea of using gravity fields to regulate MSs. They proposed a broadband lock-in absorber by combining liquid media, namely oil and seawater, as shown in Fig. 11(a). By using the different density characteristics of oil and water, two absorption states were formed by folding under the action of gravity, achieving conversion between 5.6–7.91 GHz and 4.32–5.83 GHz. This design has the advantages of low energy consumption, simple mechanism, and space resource saving, making it applicable in various fields like PCs, photonic crystals, and absorbers. In the same year, Zeng et al.[135] proposed a three-dimensional PC based on the gravity field, which achieved linear to circular polarization conversion, as shown in Fig. 11(b). The PC consisted of a three-dimensional glass cavity filled with liquid metal mercury (Hg), a copper reflector, a trench dielectric layer, and a copper patch. Under the action of the gravity field, rotating the glass cavity caused Hg to flow to different parts, forming different resonance structures and achieving different polarization conversion functions. When placed parallel to the XY plane, the axial specific band in the frequency band of 32.42–42.82 GHz (RB is 27.64%) was less than 3 dB. However, after rotation, the 3 dB axial specific band frequency was 18.88–32.86 GHz. Although these tunable electromagnetic MS designs based on gravity fields have advantages, such as wide bandwidth, high integration, space resource conservation, and simple operation, this reconfigurable technology also faces disadvantages, such as slow response speed, limited control range, and design challenges, while providing a natural and environmentally friendly control mechanism.

By analyzing the reconfigurable MS absorbers and PCs based on various tunable materials, liquid crystals, and gravity fields, it can be found that these reconfigurable design techniques have been widely studied and greatly developed, jointly promoting the development of electromagnetic MS-based absorbers and PCs. The emergence of these reconfigurable technologies effectively solves the problems of single frequency performance, poor harmony, low controllability, and inflexible functionality, which exist in early MS absorbers and PCs. However, there are still some shortcomings in these methods,
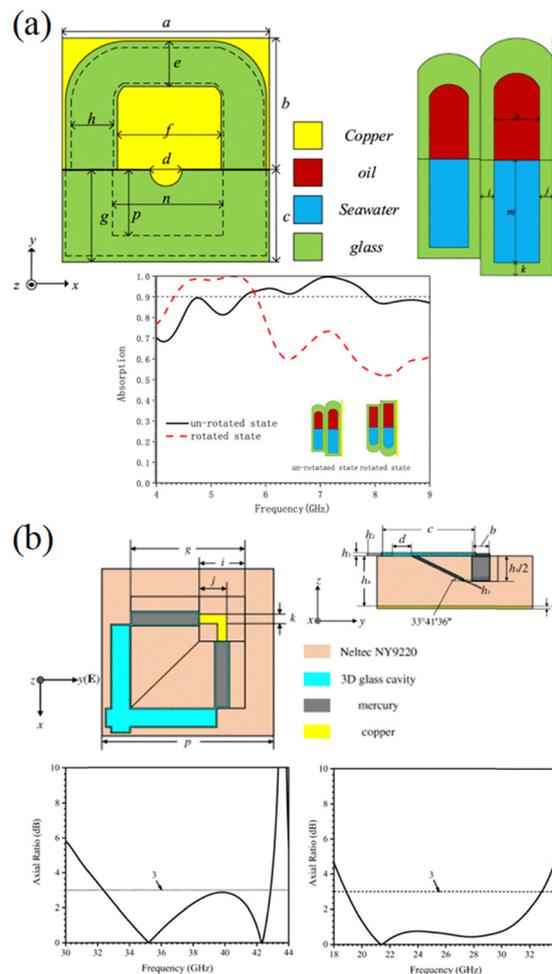

Fig. 11 (a) Broadband lock-in absorber based on the gravity field. Reproduced from ref. 134 with permission from IEEE Access, copyright 2019. (b) Three-dimensional linear-to-circular PC based on gravity field. Reproduced from ref. 135 with permission from Plasmonics, copyright 2019.

and new innovative methods and reconfigurable technologies are urgently needed.

4.2. Performance improvement technology

The technology for improving the performance of MS to some extent involves the optimization of device performance, including but not limited to research on improving the absorption or polarization conversion performance, expanding the operating frequency range, and so on. This section introduces two MS performance improvement techniques, as shown in Fig. 12, namely, intelligent optimization algorithms and structural morphology changes. The former can efficiently search for the optimal structural parameters of MSs and achieve specific performance requirements. The latter expands the application range and performance by adjusting the structural form and geometric parameters of MSs, flexibly regulating their electromagnetic properties.

In the design of large-scale and personalized MS, intelligent optimization algorithms have gradually been used to improve design efficiency and quality. The commonly used intelligent
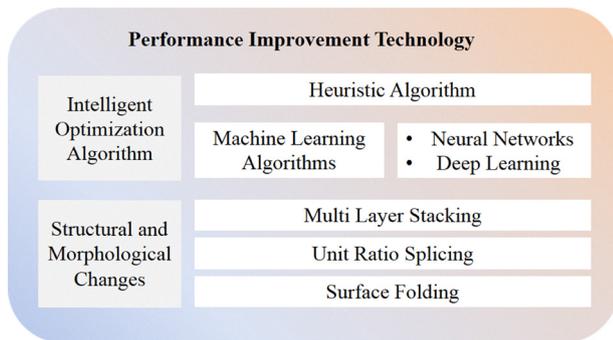
This journal is © the Owner Societies 2025

Phys. Chem. Chem. Phys., 2025, 27, 25720–25742 | 25729

Fig. 12 Performance improvement technology.

algorithms include heuristic algorithms and machine learning algorithms, which provide some flexible architectures for different design goals. Heuristic algorithms mainly include GA, PSO, Sine Cosine Algorithm (SCA), Grey Wolf Optimization (GWO), Differential Evolution Algorithm (DE), topology optimization algorithm, *etc.* common machine learning algorithms include neural networks, deep learning, *etc.* By applying intelligent algorithms, the limitations of the traditional design methods in modeling, optimization, and other aspects can be overcome, thereby improving the design speed for various applications.

At present, the method of using optimization algorithms to assist in the design of MS absorbers and PCs has been widely adopted, greatly facilitating the calculation of optimal performance corresponding to the parameters and device structure design. In 2021, Min *et al.*[136] designed a flexible broadband MS

absorber with topology optimization, as shown in Fig. 13(a). During the design process, by combining topology optimization with GA, AR exceeded 90% at 5.3–15 GHz, and broadband absorption was maintained at incident angles within 45° and 70°. The use of optimization algorithms enabled this design to have more significant broadband absorption, a lower profile, and better flexibility compared with previously reported transparent absorption materials. This method has more practical applications and demonstrates that using optimization algorithms can greatly improve device performance in the design process. In 2023, Zong *et al.*[137] designed an embedded MS solar absorber based on GA, as shown in Fig. 13(b), which operated in the ultraviolet to near-infrared wavelength range. The results showed an AR exceeding 95% at 300–2500 nm, and the average AR was above 95% at a 60° oblique angle of incidence. In 2024, Wang *et al.*[138] presented a broadband cross-polarization conversion metasurface using PSO, as shown in Fig. 13(c). The results showed that the pseudo-elliptical corner angle $\beta' \geq 0.4\pi$ and the broadband cross-polarization conversion achieved at 11.66–16.79 GHz resulted in an RB of 36.1%.

In addition, the application of machine learning in the design of MS absorbers and PCs is emerging. In 2021, Chen *et al.*[139] designed an ultra-thin broadband absorber with absorption and diffusion functions by using deep neural networks and PSO. During design, deep neural networks were used to predict reflection coefficients, and PSO was used to globally search the parameter space to find the optimal parameters for MS absorbers that meet the requirement of −10 dB backscattering suppression. In 2023, Gao *et al.*[140] designed a vector graph-based MS broadband PC using deep neural network
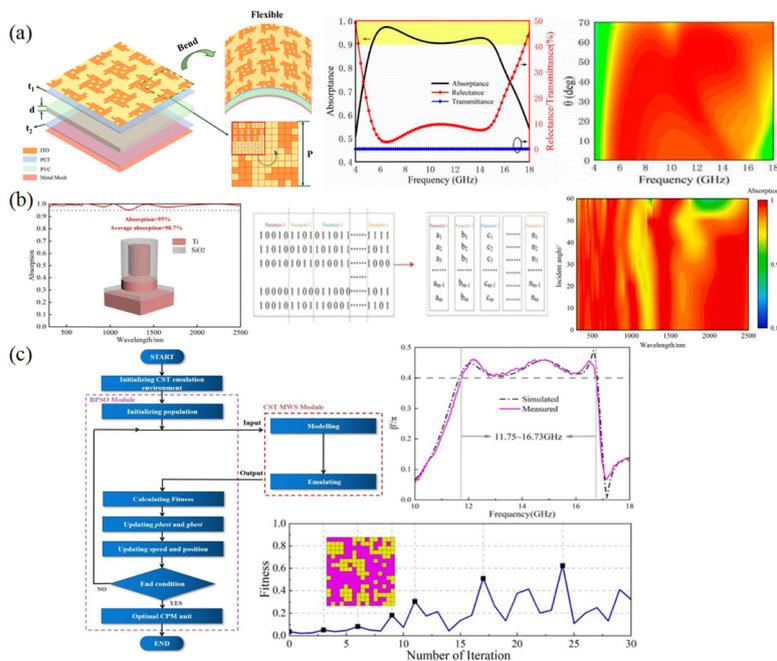

Fig. 13 (a) Flexible broadband MS absorber with topology optimization. Reproduced from ref. 136 with permission from Micromachines, copyright 2021. (b) Embedded MS solar absorber based on GA. Reproduced from ref. 137 with permission from Results in Physics, copyright 2023. (c) Broadband cross-polarization conversion MS surface designed using PSO. Reproduced from ref. 138 with permission from Materials & Design, copyright 2024.
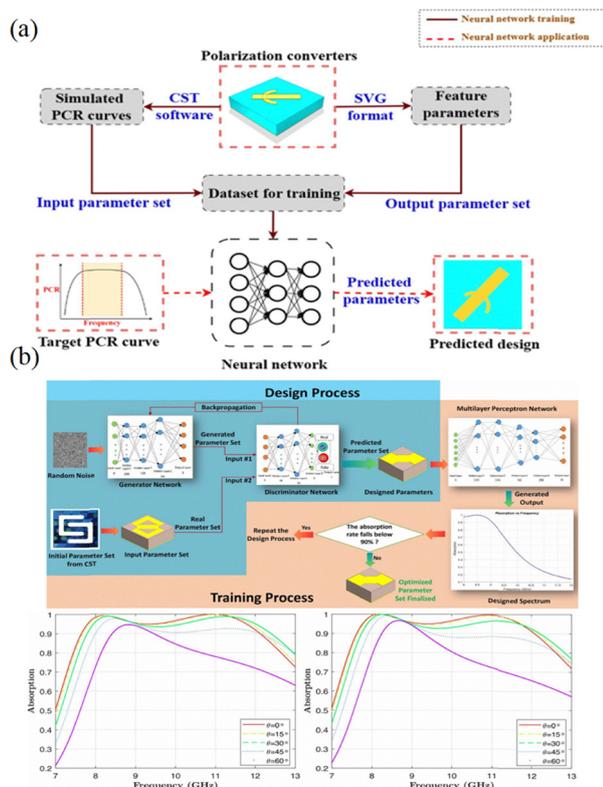
25730 | *Phys. Chem. Chem. Phys.*, 2025, **27**, 25720–25742

This journal is © the Owner Societies 2025

Fig. 14 (a) Design of an MS broadband PC using deep neural networks. Reproduced from ref. 140 with permission from Scientific Reports, copyright 2023. (b) Ultra-thin broadband absorber developed using deep learning. Reproduced from ref. 142 with permission from Scientific Reports, copyright 2025.

training methods, as shown in Fig. 14(a). The feature parameters of electromagnetic MSs extracted from vector graphics were used for deep neural network training and prediction. A PC with expected PCR spectra was successfully designed and verified through measurement. In 2024, Xiao *et al.*[141] used deep learning to assist in the design of PCs with on-demand frequency response and ultra-wideband electromagnetic scattering reduction capabilities. In the design of this PC, a combination of forward and backward convolutional neural networks was used to predict the spectral response, achieving efficient design. Then, GA was used to obtain the optimal parameters, and the designed converter reduced the radar cross-section in the ultra-wideband range of 8–37 GHz. In 2025, Shahsavaripour *et al.*[142] utilized deep learning to design thin broadband electromagnetic absorbers with polarization and angle insensitivity, as shown in Fig. 14(b). The results demonstrated a high AR of over 90% at 8–12 GHz. In addition, this MS is also suitable for TE and TM polarization, as well as wide incident angles of 0–45°.

While using optimization algorithms in the design of absorbers and PCs based on MSs, precise calculations and iterative processes can provide design ideas, simplify the design process, and quickly find optimal solutions, effectively promoting the performance of MSs. However, when the computational complexity is high (for example, large-scale or high-demand superstructure designs), a significant amount of computing resources and time is required. As mentioned above, the performance optimization of MSs based on intelligent optimization algorithms is of great significance for improving efficiency, obtaining global optimal solutions, handling multi-objective optimization, combining computational models, and promoting the development of MSs. It is an indispensable auxiliary means in the design technology of absorbers and PCs based on MSs.

In addition to utilizing intelligent optimization algorithms, changing the structural form is also an important design and optimization method that can effectively improve the performance of devices. The performance improvement technology based on structural transformation of MSs mainly includes three types, namely multi-layer stacking, unit ratio splicing, and spatial surface (folding). Through these technological means, the structural morphology and geometric parameters of MSs can be flexibly controlled, thereby fine-tuning their electromagnetic properties and further improving their performance. They are widely used in the design and performance optimization of MS-based absorbers and PCs.

Devices based on MSs can use multi-layer stacking methods to enhance electromagnetic resonance, as well as to optimize and improve the performance of MSs. In the design of PCs, a multi-layer configuration is beneficial for exciting more resonant circulating currents, which increases the magnetic field components that are conducive to polarization conversion, thereby improving performance indicators, such as polarization conversion efficiency and phase difference. Based on this optimization method, as early as 2012, Ding *et al.* proposed a pyramid-shaped MS absorber using a multi-layer stacking method, as shown in Fig. 15(a). The results demonstrated that the MS had an AR of over 90% in the 7.86–14.71 GHz range. The clever stacking of multiple layers of metal copper sheets of different sizes in the design generated a large number of absorption peaks, forming a broadband absorption frequency range. In 2016, Jia *et al.*[143] proposed an ultra-wideband and high-efficiency PC based on an MS, as shown in Fig. 15(b). The results demonstrated that the design could achieve a PCR of over 0.9 at 7.80–34.70 GHz. This design compensates for the offset of phase difference through a multi-layer structure, achieving better phase matching and obtaining efficient and continuous operating frequency bands.

Splicing unit structures of different sizes in proportion is one of the effective ways to improve the device performance and widen the frequency bands. This method utilizes the resonance frequency points of each unit structure and combines the resonance range reasonably to expand the working range, which can effectively improve the frequency bandwidth performance of MS-based absorbers and PCs. For instance, Kollatou *et al.*[144] successfully synthesized multi-band and broadband electromagnetic MS absorbers in 2013 by scaling the structural units. This design utilized the scalability and extensibility of the MS, as shown in Fig. 15(c). By combining unit structures of different sizes and placing them in composite units, multiple absorption peaks were generated, thereby extending

This journal is © the Owner Societies 2025

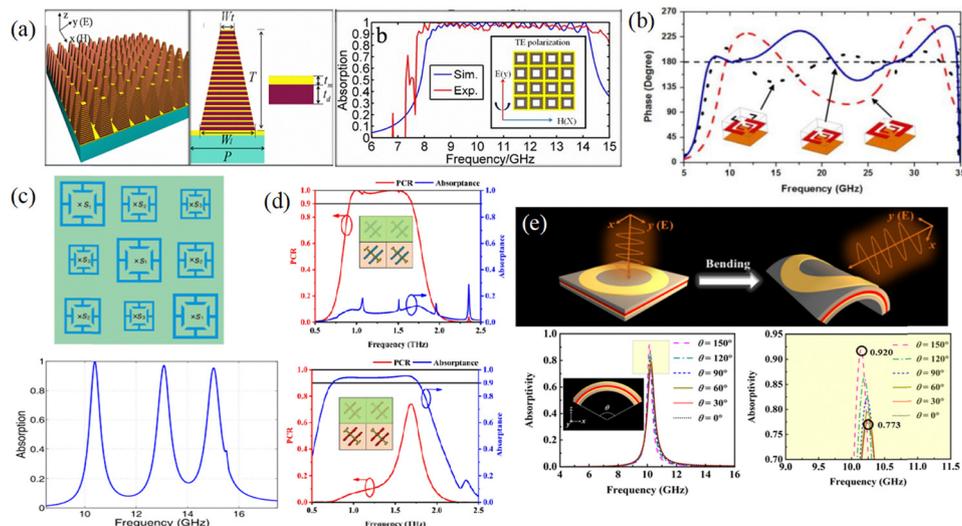*Phys. Chem. Chem. Phys.*, 2025, **27**, 25720–25742 | **25731**

Fig. 15 (a) Pyramid-shaped broadband MS absorber. Reproduced from ref. 22 with permission from Applied Physics Letters, copyright 2012. (b) Ultra-wideband high-efficiency PC based on MS. Reproduced from ref. 143 with permission from Applied Physics Letters, copyright 2016. (c) Multi-band and broadband MS absorber. Reproduced from ref. 144 with permission from Progress In Electromagnetics Research, copyright 2013. (d) Tunable MS PC using splicing technology. Reproduced from ref. 145 with permission from Applied Physics B, copyright 2021. (e) Liquid-crystal tunable curved surface absorber. Reproduced from ref. 147 with permission from Optics Express, copyright 2024.

to dual-band or even triple-band, providing innovative ideas for the design of compact dual-band electromagnetic MS absorbers. In 2021, Zhang et al.[145] presented a novel tunable MS-based PC with an expanded operating frequency band using splicing technology. As shown in Fig. 15(d), by combining four slightly different units into a super unit and applying phase compensation optimization techniques for phase matching, the operating frequency band could be significantly expanded. However, the converter, after proportional splicing, operated within the range of 0.74–1.78 THz, meeting the optimization requirements for frequency band expansion.

MSs, due to their structural plasticity, can respond to various EWs. In the design process, the spatial configuration of MS can be changed, such as curved surfaces, folds, etc., to adjust the electromagnetic response and improve device performance. In 2022, Zhu et al.[146] proposed an MS-based absorber with an origami structure. This origami absorber presented wide-angle absorption characteristics, and the absorption effect changed significantly with the adjustment of the folding state. Compared to traditional absorbers, three-dimensional origami absorbers perform better in the wide-angle range, which is up to 70°. In addition, in 2023, Bao et al.[147] proposed a liquid-crystal tunable curved electromagnetic MS designed for measuring the curvature of cylindrical surfaces. As shown in Fig. 15(e), when EWs were excited at 4–16 GHz, the absorption amplitude increased from 0.77 to 0.92, with an increase in folding curvature, indicating the effectiveness of spatial curvature in improving the performance of the MS, which can be applied in fields such as sensor design.

As mentioned, the development of MS-based absorbers and PCs using various intelligent optimization algorithms has improved device design efficiency, increased parameter optimization speed, and enhanced device intelligence. Applying various performance optimization techniques for adjusting the structural forms can further enhance the performance of devices and improve the defects in structural design. The development of these performance optimization techniques can provide designers with improved design ideas, increased optimization speed, and enhanced device performance, greatly facilitating the design process and promoting the development and application of MS-based absorbers and PCs.

By reviewing the development history of MS-based absorbers and PCs and analyzing the above techniques, we propose the following feasible strategies to enhance MS-based absorption and polarization phenomena. Firstly, to expand the absorption bandwidth of MS-based absorbers or the operational frequency range of MS-based polarization converters, techniques such as multi-layer stacking and cell arrangement with varying dimensions can be employed. Furthermore, to enhance the angular insensitivity of absorbers and converters, chiral structures may be introduced or planar models can be spatially folded, similar to origami models or conformal models. Moreover, incorporating novel composite materials, such as carbon-coated octahedral Fe_3O_4/Fe_2O_3 nanocomposites,[148] into the structure can also enhance the microwave absorption efficiency of MS-based absorbers. Besides, the addition of air vent structures[149] can also enhance the polarization conversion performance.

5. Latest research and challenges

Summarizing the previous work of researchers, it can be found that absorption and polarization based on MSs have been greatly studied and developed, but there are still innovative directions, such as asymmetric propagation, single-octave band separation, electromagnetic induced transparency (EIT),

electromagnetic induced absorption (EIA), and rasorber that need to be explored. Therefore, we analyze and explore their latest research status.

Asymmetric propagation of EWs[150,151] occurs when an EW is incident along different propagation directions, and the medium shows different transmission characteristics, including transmission, reflection, absorption and polarization conversion. The traditional method of achieving asymmetry requires the application of a magnetic field bias, which has disadvantages, such as large device size, complex structure, and difficult integration. The controllability of EWs by MSs makes it possible to design asymmetric propagation, and their advantages, such as miniaturization, simple structure, and integrability, further expand their application scope and enhance their functionality, making them a development direction with strong potential. In 2024, Lei *et al.*[152] designed broadband absorbers based on superconducting ceramic substructure photonic crystals, which achieved asymmetric absorption transmission and dual band. As shown in Fig. 16(a), the operating bandwidth was in the frequency range of 696 to 715 THz, and the RB was 2.7% when forward AR and backward transmittance rate were both more than 0.9. In the same year, they proposed an asymmetric absorption/transmission structure by using plasma substructure photonic crystals,[153] which cleverly

achieved different asymmetric propagation characteristics in the dual channel. As shown in Fig. 16(b), EWs were absorbed when incident forward and transmitted when incident backward in the 2.15–2.85 GHz range. The RB was 28% when the AR was over 0.9. EWs could be emitted in forward propagation and absorbed in backward propagation in the 7.07–7.67 GHz range, with an RB of 8.1%. This asymmetric propagation characteristic can be used to realize various irreversible electromagnetic equipment, with a lot of potential applications in optical communications, optical isolation, information transmission, stealth, and other fields. It is also an innovative and promising development direction based on the absorption and polarization of MSs.

Single-octave band separation of polarization conversion[154] refers to the process in which each frequency in the first operating frequency band has a corresponding frequency in the second frequency band that is exactly twice its value; that is, the two operating frequency bands are in a multiple relationship. In 2025, Xing *et al.*[154] proposed a dual-band linear-circular PC based on electromagnetic an MS, as shown in Fig. 17(a), which could switch the incident linearly polarized
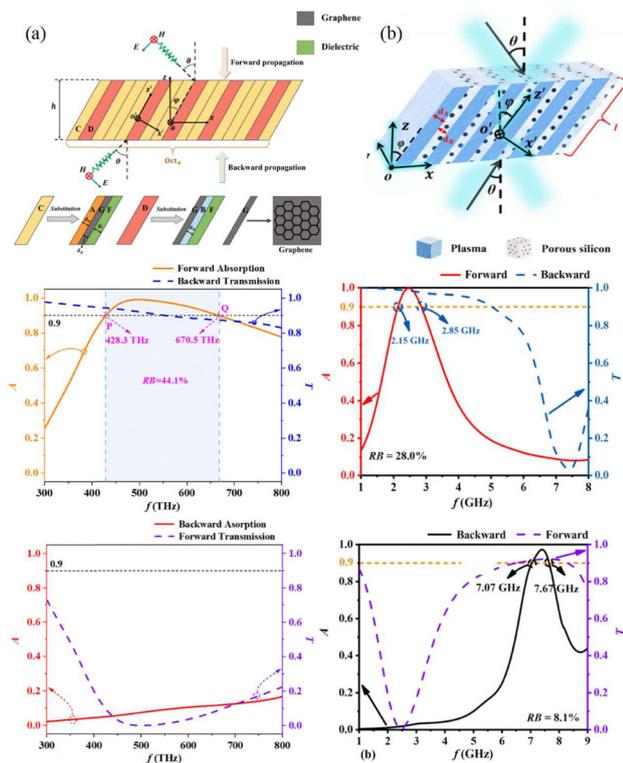

Fig. 16 (a) Broadband absorber based on superconducting ceramic substructure photonic crystals. Reproduced from ref. 152 with permission from Engineering Science and Technology, an International Journal, copyright 2024. (b) Asymmetric absorption transmission structure proposed using plasma substructure photonic crystals. Reproduced from ref. 153 with permission from Optics Express, copyright 2024.
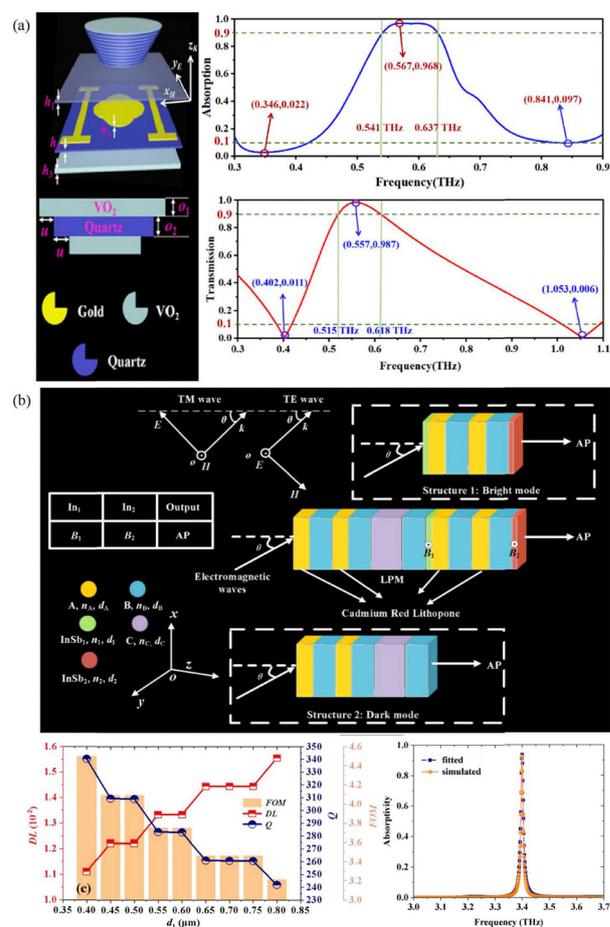
Fig. 17 (a) Dual-band PC based on MSs. Reproduced from ref. 154 with permission from Optics & Laser Technology, copyright 2024. (b) Single-band separation and reconfigurable dual-band circular PC based on liquid crystal tuning. Reproduced from ref. 155 with permission from IEEE Transactions on Instrumentation and Measurement, copyright 2025.

This journal is © the Owner Societies 2025

Phys. Chem. Chem. Phys., 2025, **27**, 25720–25742 | **25733**

waves into two orthogonal circularly polarized waves in non-adjacent frequency ranges. Specifically, the upper and lower cutoff frequencies of the second operating frequency band of the device were exactly twice those of the first frequency band. A right-handed circularly polarized wave was generated at 0.645–0.865 THz, while a left-handed circularly polarized wave was generated at 1.29–1.73 THz, with an RB of 29%. In the same year, they proposed[155] a single-octave band separation and reconfigurable dual-wideband line-to-circularly polarized converter based on liquid crystal modulation. As shown in Fig. 17(b), under zero bias, the conversion of linearly polarized waves to right-handed circularly polarized waves was achieved in the THz ranges of 0.779–0.976 and 1.429–2.085, with RB values of 22.45% and 37.34%, respectively. When the liquid crystal was fully biased, the EWs were converted into left-handed circularly polarized waves at 0.758–0.978 and 1.504–2.154 THz, with RB values of 25.35% and 35.54%, respectively. The use of MSs to design polarization converters with single-octave band separation has many outstanding advantages, such as the ability to maintain consistent output polarization while frequently switching communication between the baseband and harmonic bands. This simplifies the processing of backend signals and has strong anti-interference ability, reducing the generation of a second harmonic. Therefore, single-octave band separation is a highly promising and practical development direction based on the polarization of MSs.

EIT is defined as a quantum interference effect that creates a well-defined transmission window in the medium through coherent interactions between different energy levels, making EWs transparent within that window. On the contrary, EIA is caused by constructive interference due to quantum coherence between atomic energy levels, resulting in a dielectric window that is opaque to EWs and exhibits absorption of the probe light. The extreme experimental conditions required for the initial implementation of EIT greatly limits its practical application in daily life. However, using MSs to implement EIT and EIA not only makes the structure simple and allows easy operation but also reduces transmission losses, making it more practical and widely applicable. In 2024, Zhu et al.[156] utilized an MS to achieve the conversion of EIT to EIA. As shown in Fig. 18(a), the RB of EIT reached 18.2%. In addition, using a multi-layer stacking method, the layered stacking of vanadium dioxide circular patches with different diameters produced multiple tightly arranged resonance absorption peaks, resulting in an RB of 16.3% for EIA. In 2025, Wang et al.[157] designed a one-dimensional magnetized indium antimonide layered MS that achieved EIA and sensing function when the refractive index and thickness of the material were changed. As shown in Fig. 18(b), the refractive index range of the detectable material was from 2.4 to 2.8, and the average values of quality factor (Q), quality factor (FOM), and detection limit (DL) were 265.5, 4.308 RIU, and 0.0117 RIU, respectively. This work not only achieved coordinated EIA, but also tightly integrated logical computation with multi-parameter sensing capabilities. The significant dispersion and low loss characteristics of EIT, as well as the absorption and anomalous dispersion characteristics of EIA,
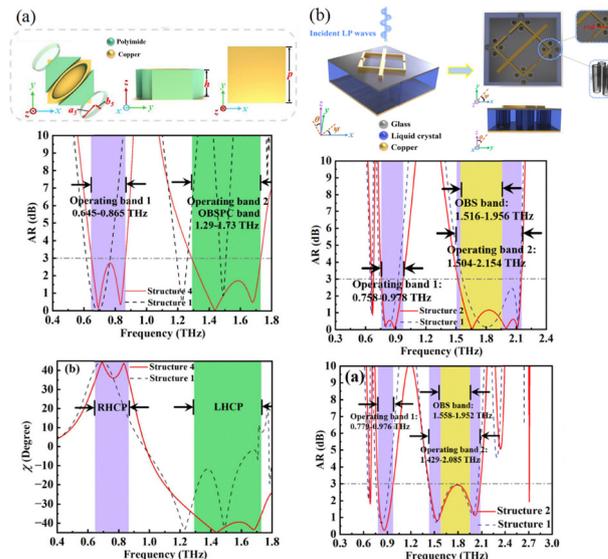

Fig. 18 (a) Broadband electromagnetic induction transparent absorption dual functional substructure based on VO₂. Reproduced from ref. 156 with permission from Optics Express, copyright 2025. (b) Magnetized indium antimonide layered MS capable of achieving EIA. Reproduced from ref. 156 with permission from Physics of Fluids, copyright 2025.

make them widely applicable in various fields, such as non-linear optics, slow light, and quantum information. The use of MS to achieve EIT and EIA remains a highly researched and practical direction based on the absorption of MSs.

Rasorber is a specialized device designed to achieve high transmission efficiency and low insertion loss in specific frequency bands while maintaining broadband absorption characteristics in other bands, enabling dual functionality of electromagnetic wave transmission and stealth in different frequency ranges. Compared with traditional absorbers, a rasorber efficiently transmits signals within designated communication windows while maintaining strong absorption in adjacent frequency bands. This dual functionality makes it an ideal choice for scenarios requiring both radar stealth and communication capabilities, such as aircraft radomes. In 2021, Jiao et al.[158] proposed a novel bipolar rasorber featuring wide absorption and transmission bands across multiple frequency bands. The device consists of a loss-frequency selective surface (FSS) with a central loading strip and metal rings in the top layer and a broadband transmission FSS as the bottom layer, separated by air, as shown in Fig. 19(a). It achieved over 80% absorption bandwidth in the 3.40–8.16 GHz range while maintaining high transmission bandwidth in the 9.03–12.01 GHz range. Notably, this configuration demonstrated exceptional performance across both absorption and transmission bands. In 2025, Kumar et al.[159] proposed a novel compact open-loop resonator-loaded rasorber that achieved both narrowband transmission and strong broadband absorption, as shown in Fig. 19(b). The top layer of the structure consisted of four centralized resistors and four improved open-loop resonators, which could absorb energy in a wide frequency range; meanwhile, the bottom layer was a multi-level coupling structure

25734 | *Phys. Chem. Chem. Phys.*, 2025, **27**, 25720–25742

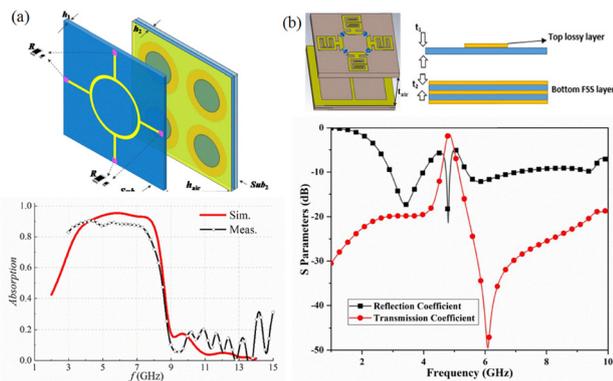This journal is © the Owner Societies 2025

Fig. 19 (a) Tunable frequency-selective rasorber. Reproduced from ref. 158 with permission from Radio Science, copyright 2021. (b) Novel compact open-loop resonator-loaded rasorber. Reproduced from ref. 159 with permission from Progress In Electromagnetics Research M, copyright 2025.

composed of an inductive lattice-folded square ring structure and an inductive lattice. Experimental results demonstrated that the proposed rasorber exhibited 124% absorption bandwidth in the 2.5 GHz to 9.5 GHz band, with 1.3 dB insertion loss at 4.8 GHz, which is the transparent window for transmission. The design innovation lies in the integration of broadband off-band absorption, narrowband on-band transmission, 50-degree angle-of-incidence stability, and dual-polarization response. Rasorbers are widely used for radar cross-section reduction and in stealth systems and military detection, making it a hot research field. Consequently, an MS-based rasorber represents a novel development that poses a significant challenge to current MS-based absorption and polarization phenomena.

Certainly, the above aspects represent only some of the possible development directions based on the absorption and polarization of MS. In addition, there can be more unknown directions and new characteristics and phenomena that remain to be studied and discovered. Importantly, absorption and polarization based on electromagnetic MSs can be developed towards functional diversification, controllability, intelligence, and integration, which has already promoted and will continue to promote the scientific progress and development of related fields. Currently, MSs have been innovatively applied in many fields, such as temperature detection and biosensing,[160] smart radiant regulator,[161] RCS reduction control[162] and logic devices for register function implementation.[163]

However, the research on absorption and polarization based on MS also faces many challenges and urgently needs further exploration from researchers. For example, combining the ultra-wideband wide-angle absorption of MS devices with non-reciprocity breaks the time reversal symmetry to achieve an asymmetric response to electromagnetic waves, thereby improving the absorption performance, polarization insensitivity, PCR and other performance parameters of the device. In addition, multifunctional devices based on MSs face challenges in improving dynamic switching stability and balancing performance metrics, such as AR, PCR, and bandwidth. Moreover,

while using MSs to design thermal radiation devices, it is necessary to address issues such as low non-reciprocal thermal radiation efficiency, low absorption and emissivity conversion rates. Applying MS to near-zero refractive index materials in the visible light band and time crystals is greatly challenging. Additionally, it can be used to combine phonon and photon effects, enabling the MS-based devices to absorb not only electromagnetic waves but also mechanical waves.

Thermal radiation is a physical process in which objects emit electromagnetic waves due to their temperature, and the intensity and wavelength distribution are determined by temperature and surface emissivity. Thermal camouflage for military stealth and counter-surveillance is achieved by modulating the thermal radiation characteristics of the target to blend with the background environment in infrared detection. Photonic thermal management further utilizes various structures to precisely control the spectrum and direction of thermal radiation, enabling efficient thermal energy utilization. It is evident that adjusting the absorption and polarization states of MS-based devices can reduce thermal radiation, thereby realizing thermal camouflage. The unique structure of MSs allows precise manipulation of electromagnetic wave characteristics and influences absorption and polarization performance, making them highly suitable for photonic thermal management. Currently, proven solutions are available for this purpose. In 2023, Jiang et al.[164] developed a seven-layer MS composed of five materials and optimized it using a GA, as shown in Fig. 20(a). Experimental results confirmed that this multi-layer thin-film structure with thermal management capabilities can be applied for infrared camouflage, demonstrating high compatibility for thermal camouflage, laser stealth, and thermal management. In 2025, Wu et al.[165] designed a multifunctional radiation-selective hierarchical MS and realized modulation of its optical properties in a wide spectral range, demonstrating exceptional incident angle and polarization stability, as shown in Fig. 20(b). Experimental results demonstrated its capability to regulate thermal radiation across different wavelength bands. For instance, suppressing the target's infrared radiation in specific bands can achieve efficient infrared stealth. Meanwhile, high emissivity in another band significantly enhances the thermal radiation efficiency. Notably, it exhibited low reflectivity in the 8–14 μm band, which substantially improved the laser stealth performance. This demonstrates the feasibility of using MSs for radiation cooling, thermal camouflage, and photonic thermal management, with significant potential in applications such as thermal imaging, military detection, and stealth technology.

In the future, MS-based devices will see advancements in asymmetric propagation, single-octave band separation, EIT, EIA, and rasorber applications. When applying MS in thermal radiation device design, challenges such as low non-reciprocal thermal radiation efficiency and insufficient absorption-emission conversion rates must be addressed. For instance, a viable approach involves combining the ultra-wideband wide-angle absorption characteristics of MS devices with non-reciprocity principles to break time-reversal symmetry, enabling asymmetric electromagnetic wave responses that significantly
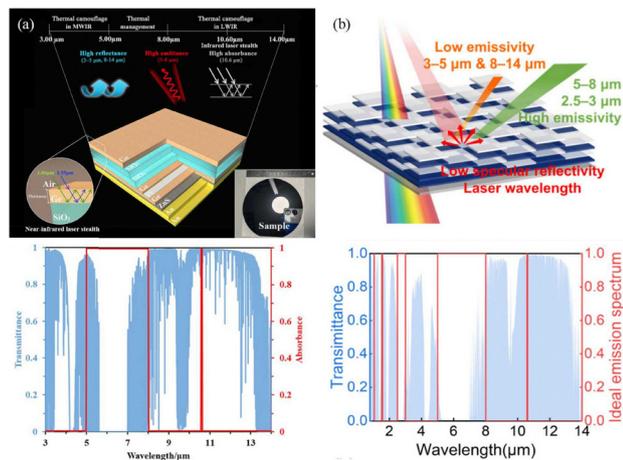
This journal is © the Owner Societies 2025

Phys. Chem. Chem. Phys., 2025, **27**, 25720–25742 | **25735**

Fig. 20 (a) Seven-layer MS composed of five materials. Reproduced from ref. 164 with permission from Nanophotonics, copyright 2023. (b) Multifunctional radiation-selective hierarchical MS. Reproduced from ref. 165 with permission from Photonics, copyright 2025.

enhance key performance indicators like absorption efficiency, polarization insensitivity, and PCR. However, devices based on MSs still face challenges in optimizing dynamic switching stability, phase control rate, and bandwidth balance. Furthermore, applying MSs in the design of thermal radiation devices has emerged as a promising research direction. This approach holds significant practical value and research significance in military stealth applications, enabling thermal radiation, thermal camouflage, and photonic thermal management. However, this technology also faces many significant challenges, such as applying MS to achieve near zero refractive index, time crystals, and phonon photon synergistic effects, which may be significant research directions for future exploration.

6. Conclusions

In summary, since their theoretical conception and experimental validation, MSs have attracted extensive research interest due to their unique properties, which transcend the limitations of conventional materials. These structures have emerged as a prominent research focus, leading to the development and deployment of various MS-based devices. Among these, absorbers and PCs have drawn particular attention for their distinctive characteristics and have seen remarkable progress. Both play crucial roles in a wide range of electromagnetic, communication, and optoelectronic applications, and are widely employed in fields such as communications, military stealth, and aerospace. With ongoing advancements in the information age, MS-based devices are increasingly evolving toward tunability, intelligence, interdisciplinary integration, and miniaturization.

Compared with earlier works in the field, this review provides clear definitions and explanations of MSs, classifying them into three categories: photonic crystals, electromagnetic metasurfaces, and electromagnetic metamaterials. It systematically outlines the evolution of MS-based absorbers and PCs,

emphasizing key improvements in areas such as absorption efficiency, operational bandwidth, polarization conversion efficiency, and functional versatility. Research in MS design methodologies can offer valuable pathways for overcoming the current developmental bottlenecks. This article summarizes effective design strategies, with a focus on reconfigurable technologies and performance enhancement techniques applicable to both absorbers and PCs. Three types of reconfigurable technologies are discussed, along with performance improvement approaches explored through intelligent optimization algorithms and structural modifications. Specifically, three structural enhancement techniques, namely, multi-layer stacking, multi-unit tiling, and spatial folding/origami structures, are highlighted. These methods enable flexible control over the geometry and configuration of MSs, allowing precise tuning of their electromagnetic responses and overall performance optimization. Furthermore, the review analyzes the current research landscape in MS-based absorption and polarization control, introducing designs based on asymmetric propagation, frequency-selective separation, EIT, and EIA. Finally, we discuss the challenges and opportunities facing MS technology, outlining promising future directions, such as non-reciprocal devices, thermal radiation control, time crystals, and hybrid phonon–photon phenomena.

Author contributions

Xue-Fang He: investigation, data curation, writing – original draft. Hai-Feng Zhang: conceptualization, methodology, supervision, writing – review & editing.

Conflicts of interest

The authors declare that they have no known competing financial interests or personal relationships that could have appeared to influence the work reported in this paper.

Data availability

The data that support the findings of this study are available from the corresponding author upon reasonable request.

Acknowledgements

Notes and references

1 J. D. Joannopoulos, P. R. Villeneuve and S. Fan, Photonic crystals, *Solid State Commun.*, 1997, **102**(2–3), 165–173.

2 A. Sihvola, Metamaterials in electromagnetics, *Metamaterials*, 2007, **1**(1), 2–11.

25736 | *Phys. Chem. Chem. Phys.*, 2025, **27**, 25720–25742

This journal is © the Owner Societies 2025

3 D. R. Smith, J. B. Pendry and M. C. Wiltshire, Metamaterials and negative refractive index, *Science*, 2004, **305**(5685), 788–792.

4 M. Bayindir, K. Aydin, E. Ozbay, P. Markoš and C. Soukoulis, Transmission properties of composite metamaterials in free space, *Appl. Phys. Lett.*, 2002, **81**(1), 120–122.

5 Y. Yao, Z. Liao, Z. Liu, X. Liu, J. Zhou and G. Liu, *et al.*, Recent progresses on metamaterials for optical absorption and sensing: A review, *J. Phys. D: Appl. Phys.*, 2021, **54**(11), 113002.

6 X. Ni, Z. J. Wong, M. Mrejen, Y. Wang and X. Zhang, An ultrathin invisibility skin cloak for visible light, *Science*, 2015, **349**(6254), 1310–1314.

7 H.-T. Chen, A. J. Taylor and N. Yu, A review of metasurfaces: physics and applications, *Rep. Prog. Phys.*, 2016, **79**(7), 076401.

8 K. Fan and W. J. Padilla, Dynamic electromagnetic metamaterials, *Mater. Today*, 2015, **18**(1), 39–50.

9 T. J. Cui, Microwave metamaterials—from passive to digital and programmable controls of electromagnetic waves, *J. Opt.*, 2017, **19**(8), 084004.

10 J. B. Pendry, A. Holden, W. Stewart and I. Youngs, Extremely low frequency plasmons in metallic mesostructures, *Phys. Rev. Lett.*, 1996, **76**(25), 4773.

11 J. B. Pendry, A. J. Holden, D. J. Robbins and W. J. Stewart, Magnetism from conductors and enhanced nonlinear phenomena, *IEEE Trans. Microwave Theory Tech.*, 1999, **47**(11), 2075–2084.

12 R. A. Shelby, D. R. Smith and S. Schultz, Experimental verification of a negative index of refraction, *Science*, 2001, **292**(5514), 77–79.

13 J. B. Pendry, D. Schurig and D. R. Smith, Controlling electromagnetic fields, *Science*, 2006, **312**(5781), 1780–1782.

14 D. R. Smith, J. J. Mock, A. Starr and D. Schurig, Gradient index metamaterials, *Phys. Rev. E: Stat., Nonlinear, Soft Matter Phys.*, 2005, **71**(3), 036609.

15 A. Alù, Mantle cloak: Invisibility induced by a surface, *Phys. Rev. B: Condens. Matter Mater. Phys.*, 2009, **80**(24), 245115.

16 T. Bückmann, M. Thiel, M. Kadic, R. Schittny and M. Wegener, An elasto-mechanical unfeelability cloak made of pentamode metamaterials, *Nat. Commun.*, 2014, **5**(1), 4130.

17 H. Chu, Q. Li, B. Liu, J. Luo, S. Sun and Z. H. Hang, *et al.*, A hybrid invisibility cloak based on integration of transparent metasurfaces and zero-index materials, *Light: Sci. Appl.*, 2018, **7**(1), 50.

18 S. Islam, M. Hasan and M. Faruque, A new metamaterial-based wideband rectangular invisibility cloak, *Appl. Phys. A*, 2018, **124**(2), 160.

19 R. Melik, E. Unal, N. K. Perkgoz, C. Puttlitz and H. V. Demir, Metamaterial-based wireless strain sensors, *Appl. Phys. Lett.*, 2009, **95**, 1.

20 W. Wang, F. Yan, S. Tan, H. Zhou and Y. Hou, Ultrasensitive terahertz metamaterial sensor based on vertical split ring resonators, *Photonics Res.*, 2017, **5**(6), 571–577.

21 W. Xu, L. Xie and Y. Ying, Mechanisms and applications of terahertz metamaterial sensing: a review, *Nanoscale*, 2017, **9**(37), 13864–13878.

22 F. Ding, Y. Cui, X. Ge, Y. Jin and S. He, Ultra-broadband microwave metamaterial absorber, *Appl. Phys. Lett.*, 2012, **100**, 10.

23 N. I. Landy, S. Sajuyigbe, J. J. Mock, D. R. Smith and W. J. Padilla, Perfect metamaterial absorber, *Phys. Rev. Lett.*, 2008, **100**(20), 207402.

24 H. Tao, N. I. Landy, C. M. Bingham, X. Zhang, R. D. Averitt and W. J. Padilla, A metamaterial absorber for the terahertz regime: design, fabrication and characterization, *Opt. Express*, 2008, **16**(10), 7181–7188.

25 P. Yu, L. V. Besteiro, Y. Huang, J. Wu, L. Fu and H. H. Tan, *et al.*, Broadband metamaterial absorbers, *Adv. Opt. Mater.*, 2019, **7**(3), 1800995.

26 X. Jing, X. Gui, P. Zhou and Z. Hong, Physical explanation of Fabry–Pérot cavity for broadband bilayer metamaterials polarization converter, *J. Light Technol.*, 2018, **36**(12), 2322–2327.

27 D. L. Markovich, A. Andryieuski, M. Zalkovskij, R. Malureanu and A. V. Lavrinenko, Metamaterial polarization converter analysis: limits of performance, *Appl. Phys. B*, 2013, **112**(2), 143–152.

28 X. Yu, X. Gao, W. Qiao, L. Wen and W. Yang, Broadband tunable polarization converter realized by graphene-based metamaterial, *IEEE Photonics Technol. Lett.*, 2016, **28**(21), 2399–2402.

29 J. Zi, Q. Xu, Q. Wang, C. Tian, Y. Li and X. Zhang, *et al.*, Antireflection-assisted all-dielectric terahertz metamaterial polarization converter, *Appl. Phys. Lett.*, 2018, **113**, 10.

30 C. Milias, R. B. Andersen, P. I. Lazaridis, Z. D. Zaharis, B. Muhammad and J. T. Kristensen, *et al.*, Metamaterial-inspired antennas: A review of the state of the art and future design challenges, *IEEE Access*, 2021, **9**, 89846–89865.

31 Y. Liu and X. Zhao, Perfect absorber metamaterial for designing low-RCS patch antenna, *IEEE Antennas Wirel. Propag. Lett.*, 2014, **13**, 1473–1476.

32 Y. Liu, Y. Hao, K. Li and S. Gong, Radar cross section reduction of a microstrip antenna based on polarization conversion metamaterial, *IEEE Antennas Wirel. Propag. Lett.*, 2015, **15**, 80–83.

33 C. M. Watts, X. Liu and W. J. Padilla, Metamaterial electromagnetic wave absorbers, *Adv. Mater.*, 2012, **24**(23), OP98–OP120.

34 Q. Zheng, C. Guo and J. Ding, Wideband metasurface-based reflective polarization converter for linear-to-linear and linear-to-circular polarization conversion, *IEEE Antennas Wirel. Propag. Lett.*, 2018, **17**(8), 1459–1463.

35 Y.-Z. Ran, L.-H. Shi, J.-B. Wang, S.-B. Wang, G.-M. Wang and J.-G. Liang, Ultra-wideband linear-to-circular polarization converter with ellipse-shaped metasurfaces, *Opt. Commun.*, 2019, **451**, 124–128.

36 J. J. Gil, A. Norrman, A. T. Friberg and T. Setälä, Polarimetric purity and the concept of degree of polarization, *Phys. Rev. A*, 2018, **97**(2), 023838.

37 Y. Gao, H. Jing, J. Wang, J. Kang, L. Zhao and L. Chen, *et al.*, A transparent broadband flexible metamaterial absorber for radar infrared-compatible stealth, *J. Phys. D: Appl. Phys.*, 2024, **57**(15), 155102.

38 J. Kang, Z. Qu, J. Duan, H. Jing, J. Hao and C. Song, *et al.*, Multispectral flexible ultrawideband metamaterial absorbers for radar stealth and visible light transparency, *Opt. Mater.*, 2023, **135**, 113351.

39 C. Quan, J. Zou, C. Guo, W. Xu, Z. Zhu and J. Zhang, High-temperature resistant broadband infrared stealth metamaterial absorber, *Opt. Laser Technol.*, 2022, **156**, 108579.

40 C. Xu, S. Qu, Y. Pang, J. Wang, M. Yan and J. Zhang, *et al.*, Metamaterial absorber for frequency selective thermal radiation, *Infrared Phys. Technol.*, 2018, **88**, 133–138.

41 Y. Zhang, H. Dong, N. Mou, L. Chen, R. Li and L. Zhang, High-performance broadband electromagnetic interference shielding optical window based on a metamaterial absorber, *Opt. Express*, 2020, **28**(18), 26836–26849.

42 Q. Lv, Z. Peng, H. Pei, X. Zhang, Y. Chen and H. Zhang, *et al.*, 3D printing of periodic porous metamaterials for tunable electromagnetic shielding across broad frequencies, *Nano-Micro Lett.*, 2024, **16**(1), 279.

43 J. Zhou, P. Zhang, J. Han, L. Li and Y. Huang, Metamaterials and metasurfaces for wireless power transfer and energy harvesting, *Proc. IEEE*, 2021, **110**(1), 31–55.

44 Y. Wei, J. Duan, H. Jing, Z. Lyu, J. Hao and Z. Qu, *et al.*, A multiband, polarization-controlled metasurface absorber for electromagnetic energy harvesting and wireless power transfer, *IEEE Trans. Microwave Theory Tech.*, 2022, **70**(5), 2861–2871.

45 Y. Wu, S. Tan, Y. Zhao, L. Liang, M. Zhou and G. Ji, Broadband multispectral compatible absorbers for radar, infrared and visible stealth application, *Prog. Mater. Sci.*, 2023, **135**, 101088.

46 N. Han, Z. Chen, C. Lim, B. Ng and M. Hong, Broadband multi-layer terahertz metamaterials fabrication and characterization on flexible substrates, *Opt. Express*, 2011, **19**(8), 6990–6998.

47 M. J. Dicken, K. Aydin, I. M. Pryce, L. A. Sweatlock, E. M. Boyd and S. Walavalkar, *et al.*, Frequency tunable near-infrared metamaterials based on VO2 phase transition, *Opt. Express*, 2009, **17**(20), 18330–18339.

48 F. Wang, H. Liu, T. Li, Z. Dong, S. Zhu and X. Zhang, Metamaterial of rod pairs standing on gold plate and its negative refraction property in the far-infrared frequency regime, *Phys. Rev. E: Stat., Nonlinear, Soft Matter Phys.*, 2007, **75**(1), 016604.

49 R. Maas, J. Parsons, N. Engheta and A. Polman, Experimental realization of an epsilon-near-zero metamaterial at visible wavelengths, *Nat. Photonics*, 2013, **7**(11), 907–912.

50 C. Guo, F. Liu, S. Chen, C. Feng and Z. Zeng, Advances on exploiting polarization in wireless communications: Channels, technologies, and applications, *IEEE Commun. Surv. Tutor.*, 2016, **19**(1), 125–166.

51 W. Liu, J. C. Ke, C. Xiao, L. Zhang, Q. Cheng and T. J. Cui, Broadband polarization-reconfigurable converter using active metasurfaces, *IEEE Trans. Antennas Propag.*, 2023, **71**(4), 3725–3730.

52 S. Pandit, A. Mohan and P. Ray, Low-RCS low-profile four-element MIMO antenna using polarization conversion metasurface, *IEEE Antennas Wirel. Propag. Lett.*, 2020, **19**(12), 2102–2106.

53 Y. Huang, L. Yang, J. Li, Y. Wang and G. Wen, Polarization conversion of metasurface for the application of wide band low-profile circular polarization slot antenna, *Appl. Phys. Lett.*, 2016, **109**, 5.

54 Y. Zheng, Y. Zhou, J. Gao, X. Cao, H. Yang and S. Li, *et al.*, Ultra-wideband polarization conversion metasurface and its application cases for antenna radiation enhancement and scattering suppression, *Sci. Rep.*, 2017, **7**(1), 16137.

55 K. Li, Y. Liu, Y. Jia and Y. Guo, A circularly polarized high-gain antenna with low RCS over a wideband using chessboard polarization conversion metasurfaces, *IEEE Trans. Antennas Propag.*, 2017, **65**(8), 4288–4292.

56 Y. Liang, Q. Tan, W. Zhou, X. Zhou, Z. Wang and G. Zhou, *et al.*, Refractive index sensing utilizing tunable polarization conversion efficiency with dielectric metasurface, *J. Light Technol.*, 2020, **39**(2), 682–687.

57 E. Shokati, S. Asgari and N. Granpayeh, Dual-band polarization-sensitive graphene chiral metasurface and its application as a refractive index sensor, *IEEE Sens. J.*, 2019, **19**(21), 9991–9996.

58 Z.-Y. Zhang, F. Fan, T.-F. Li, Y.-Y. Ji and S.-J. Chang, Terahertz polarization conversion and sensing with double-layer chiral metasurface, *Chin. Phys. B*, 2020, **29**(7), 078707.

59 Y. Qi, B. Zhang, C. Liu and X. Deng, Ultra-broadband polarization conversion meta-surface and its application in polarization converter and RCS reduction, *IEEE Access*, 2020, **8**, 116675.

60 J. Wei, Y. Qi, B. Zhang, J. Ding, W. Liu and X. Wang, Research on beam manipulate and RCS reduction based on terahertz ultra-wideband polarization conversion metasurface, *Opt. Commun.*, 2022, **502**, 127425.

61 X. Zang, F. Dong, F. Yue, C. Zhang, L. Xu and Z. Song, *et al.*, Polarization encoded color image embedded in a dielectric metasurface, *Adv. Mater.*, 2018, **30**(21), 1707499.

62 R. Zhao, X. Xiao, G. Geng, X. Li, J. Li and X. Li, *et al.*, Polarization and Holography Recording in Real-and k-Space Based on Dielectric Metasurface, *Adv. Funct. Mater.*, 2021, **31**(27), 2100406.

63 J. Rhee, Y. Yoo, K. Kim, Y. Kim and Y. Lee, Metamaterial-based perfect absorbers, *J. Electromagn. Wave Appl.*, 2014, **28**(13), 1541–1580.

64 F. Dincer, M. Karaaslan and C. Sabah, Design and analysis of perfect metamaterial absorber in GHz and THz frequencies, *J. Electromagn. Wave Appl.*, 2015, **29**(18), 2492–2500.

65 G. Duan, J. Schalch, X. Zhao, J. Zhang, R. Averitt and X. Zhang, Identifying the perfect absorption of metamaterial absorbers, *Phys. Rev. B*, 2018, **97**(3), 035128.

66 P. F. Pai, H. Peng and S. Jiang, Acoustic metamaterial beams based on multi-frequency vibration absorbers, *Int. J. Mech. Sci.*, 2014, **79**, 195–205.

67 J. Wang, X. Ding, X. Huang, J. Wu, Y. Li and H. Yang, Metamaterials absorber for multiple frequency points within 1 GHz, *Phys. Scr.*, 2020, **95**(6), 065505.

25738 | *Phys. Chem. Chem. Phys.*, 2025, **27**, 25720–25742

This journal is © the Owner Societies 2025

68 Y. J. Kim, Y. J. Yoo, K. W. Kim, J. Y. Rhee, Y. H. Kim and Y. Lee, Dual broadband metamaterial absorber, *Opt. Express*, 2015, **23**(4), 3861–3868.

69 B. X. Wang, C. Xu, G. Duan, W. Xu and F. Pi, Review of broadband metamaterial absorbers: from principles, design strategies, and tunable properties to functional applications, *Adv. Funct. Mater.*, 2023, **33**(14), 2213818.

70 M. Li, H.-L. Yang, X.-W. Hou, Y. Tian and D.-Y. Hou, Perfect metamaterial absorber with dual bands, *Prog. Electromagn. Res.*, 2010, **108**, 37–49.

71 S. Shrestha, Y. Wang, A. C. Overvig, M. Lu, A. Stein and L. D. Negro, *et al.*, Indium tin oxide broadband metasurface absorber, *ACS Photonics*, 2018, **5**(9), 3526–3533.

72 S. Fan and Y. Song, Ultra-wideband flexible absorber in microwave frequency band, *Materials*, 2020, **13**(21), 4883.

73 Y. Kim and J.-H. Lee, Broadband metasurface absorber based on an optimal combination of copper tiles and chip resistors, *Materials*, 2023, **16**(7), 2692.

74 B.-Y. Wang, S.-B. Liu, B.-R. Bian, Z.-W. Mao, X.-C. Liu and B. Ma, *et al.*, A novel ultrathin and broadband microwave metamaterial absorber, *J. Appl. Phys.*, 2014, **116**, 9.

75 M. R. Soheilifar, R. A. Sadeghzadeh and H. Gobadi, Design and fabrication of a metamaterial absorber in the microwave range, *Microw. Opt. Technol. Lett.*, 2014, **56**(8), 1748–1752.

76 C. Chen, M. Chai, M. Jin and T. He, Terahertz metamaterial absorbers, *Adv. Mater. Technol.*, 2022, **7**(5), 2101171.

77 G. Yao, F. Ling, J. Yue, C. Luo, J. Ji and J. Yao, Dual-band tunable perfect metamaterial absorber in the THz range, *Opt. Express*, 2016, **24**(2), 1518–1527.

78 L. Lei, S. Li, H. Huang, K. Tao and P. Xu, Ultra-broadband absorber from visible to near-infrared using plasmonic metamaterial, *Opt. Express*, 2018, **26**(5), 5686–5693.

79 F. Ding, J. Dai, Y. Chen, J. Zhu, Y. Jin and S. I. Bozhevolnyi, Broadband near-infrared metamaterial absorbers utilizing highly lossy metals, *Sci. Rep.*, 2016, **6**(1), 39445.

80 R. Parvaz and H. Karami, Far-infrared multi-resonant graphene-based metamaterial absorber, *Opt. Commun.*, 2017, **396**, 267–274.

81 Y. Zhou, Z. Qin, Z. Liang, D. Meng, H. Xu and D. R. Smith, *et al.*, Ultra-broadband metamaterial absorbers from long to very long infrared regime, *Light: Sci. Appl.*, 2021, **10**(1), 138.

82 T. S. Tuan and N. T. Q. Hoa, Numerical study of an efficient broadband metamaterial absorber in visible light region, *IEEE Photonics J.*, 2019, **11**(3), 1–10.

83 M. Li, B. Muneer, Z. Yi and Q. Zhu, A broadband compatible multispectral metamaterial absorber for visible, near-infrared, and microwave bands, *Adv. Opt. Mater.*, 2018, **6**(9), 1701238.

84 J. Zhu, Z. Ma, W. Sun, F. Ding, Q. He and L. Zhou, *et al.*, Ultra-broadband terahertz metamaterial absorber, *Appl. Phys. Lett.*, 2014, **105**, 2.

85 P. Wu, Y. Wang, Z. Yi, Z. Huang, Z. Xu and P. Jiang, A near-infrared multi-band perfect absorber based on 1D gold grating Fabry-Perot structure, *IEEE Access*, 2020, **8**, 72742–72748.

86 S. I. Sayed, K. Mahmoud and R. I. Mubarak, Design and optimization of broadband metamaterial absorber based on manganese for visible applications, *Sci. Rep.*, 2023, **13**(1), 11937.

87 B. Zhu, Z. Wang, C. Huang, Y. Feng, J. Zhao and T. Jiang, Polarization insensitive metamaterial absorber with wide incident angle, *Prog. Electromagn. Res.*, 2010, **101**, 231–239.

88 T. T. Nguyen and S. Lim, Design of metamaterial absorber using eight-resistive-arm cell for simultaneous broadband and wide-incidence-angle absorption, *Sci. Rep.*, 2018, **8**(1), 6633.

89 X. Wang, Y. Liang, L. Wu, J. Guo, X. Dai and Y. Xiang, Multi-channel perfect absorber based on a one-dimensional topological photonic crystal heterostructure with graphene, *Opt. Lett.*, 2018, **43**(17), 4256–4259.

90 H. Jiang, W. Yang, R. Li, S. Lei, B. Chen and H. Hu, *et al.*, A conformal metamaterial-based optically transparent microwave absorber with high angular stability, *IEEE Antennas Wirel. Propag. Lett.*, 2021, **20**(8), 1399–1403.

91 S. Zheng, M. Gu, G. Feng, M. Zheng, T. Zhao and X. Jing, *Design of a Polarization-Insensitive and Wide-Angle Triple-Band Metamaterial Absorber*. MDPI, 2025, p. 386.

92 J. Hao, Y. Yuan, L. Ran, T. Jiang, J. A. Kong and C. T. Chan, *et al.*, Manipulating electromagnetic wave polarizations by anisotropic metamaterials, *Phys. Rev. Lett.*, 2007, **99**(6), 063908.

93 J. Xu, R. Li, J. Qin, S. Wang and T. Han, Ultra-broadband wide-angle linear polarization converter based on H-shaped metasurface, *Opt. Express*, 2018, **26**(16), 20913–20919.

94 Y. Guo, M. Xiao, Y. Zhou and S. Fan, Arbitrary polarization conversion with a photonic crystal slab, *Adv. Opt. Mater.*, 2019, **7**(14), 1801453.

95 S. Hafeez, J. Yu, F. A. Umrani, W. Yun and M. Ishfaq, A multiband and multifunctional metasurface for linear and circular polarization conversion in reflection modes, *Crystals*, 2024, **14**(3), 266.

96 X. Huang, D. Yang and H. Yang, Multiple-band reflective polarization converter using U-shaped metamaterial, *J. Appl. Phys.*, 2014, **115**, 10.

97 R. Dutta, J. Ghosh, Z. Yang and X. Zhang, Multi-band multi-functional metasurface-based reflective polarization converter for linear and circular polarizations, *IEEE Access*, 2021, **9**, 152738.

98 X. Liu, J. Zhang, W. Li, R. Lu, L. Li and Z. Xu, *et al.*, Three-band polarization converter based on reflective metasurface, *IEEE Antennas Wirel. Propag. Lett.*, 2016, **16**, 924–927.

99 B. Lin, J. Guo, Y. Ma, W. Wu, X. Duan and Z. Wang, *et al.*, Design of a wideband transmissive linear-to-circular polarization converter based on a metasurface, *Appl. Phys. A*, 2018, **124**(10), 715.

100 A. K. Fahad, C. Ruan, S. A. Ali, R. Nazir, T. U. Haq and S. Ullah, *et al.*, Triband ultrathin polarization converter for X/Ku/Ka-band microwave transmission, *IEEE Microw. Wirel. Compon. Lett.*, 2020, **30**(4), 351–354.

101 M. Chandra, D. Samantaray, M. Thottappan and S. Bhattacharyya, A broadband transmissive type metasurface

This journal is © the Owner Societies 2025

Phys. Chem. Chem. Phys., 2025, **27**, 25720–25742 | **25739**

cross-polarization converter for EMC application, *IEEE Trans. Electromagn. Compat.*, 2022, **65**(1), 186–194.

102 X. Gao, X. Han, W.-P. Cao, H. O. Li, H. F. Ma and T. J. Cui, Ultrawideband and high-efficiency linear polarization converter based on double V-shaped metasurface, *IEEE Trans. Antennas Propag.*, 2015, **63**(8), 3522–3530.

103 Y. Guo, J. Xu, C. Lan and K. Bi, Broadband and high-efficiency linear polarization converter based on reflective metasurface, Engineered, *Science*, 2021, **14**(2), 39–45.

104 B. Lin, J. Guo, Y. Ma, W. Wu, X. Duan and Z. Wang, *et al.*, Design of a wideband transmissive linear-to-circular polarization converter based on a metasurface, *Appl. Phys. A*, 2018, **124**(10), 715.

105 S. Bang, J. Kim, G. Yoon, T. Tanaka and J. Rho, Recent advances in tunable and reconfigurable metamaterials, *Micromachines*, 2018, **9**(11), 560.

106 H. Jeong, D. H. Le, D. Lim, R. Phon and S. Lim, Reconfigurable metasurfaces for frequency selective absorption, *Adv. Opt. Mater.*, 2020, **8**(13), 1902182.

107 S. Xiao, T. Wang, T. Liu, C. Zhou, X. Jiang and J. Zhang, Active metamaterials and metadevices: a review, *J. Phys. D: Appl. Phys.*, 2020, **53**(50), 503002.

108 A. K. Geim and K. S. Novoselov, The rise of graphene, *Nat. Mater.*, 2007, **6**(3), 183–191.

109 D. Usachov, V. K. Adamchuk, D. Haberer, A. Grüneis, H. Sachdev and A. B. Preobrajenski, *et al.*, Quasifreestanding single-layer hexagonal boron nitride as a substrate for graphene synthesis, *Phys. Rev. B: Condens. Matter Mater. Phys.*, 2010, **82**(7), 075415.

110 X. Wan, G. Long, L. Huang and Y. Chen, Graphene–a promising material for organic photovoltaic cells, *Adv. Mater.*, 2011, **23**(45), 5342–5358.

111 S. Das, D. Pandey, J. Thomas and T. Roy, The role of graphene and other 2D materials in solar photovoltaics, *Adv. Mater.*, 2019, **31**(1), 1802722.

112 R. You, Y. Q. Liu, Y. L. Hao, D. D. Han, Y. L. Zhang and Z. You, Laser fabrication of graphene-based flexible electronics, *Adv. Mater.*, 2020, **32**(15), 1901981.

113 C. Liu, L. Qi and X. Zhang, Broadband graphene-based metamaterial absorbers, *AIP Adv.*, 2018, **8**, 1.

114 R. Zhang, B. You, S. Wang, K. Han, X. Shen and W. Wang, Broadband and switchable terahertz polarization converter based on graphene metasurfaces, *Opt. Express*, 2021, **29**(16), 24804–24815.

115 J. B. Goodenough, The two components of the crystallographic transition in VO2, *J. Solid State Chem.*, 1971, **3**(4), 490–500.

116 J. M. Wu and L. B. Liou, Room temperature photo-induced phase transitions of VO2 nanodevices, *J. Mater. Chem.*, 2011, **21**(14), 5499–5504.

117 L. Bai, Q. Li, S. A. Corr, Y. Meng, C. Park and S. V. Sinogeikin, *et al.*, Pressure-induced phase transitions and metallization in VO_2, *Phys. Rev. B: Condens. Matter Mater. Phys.*, 2015, **91**(10), 104110.

118 L. Pósa, G. Molnár, B. Kalas, Z. Baji, Z. Czigány and P. Petrik, *et al.*, A rational fabrication method for low switching-temperature VO_2, *Nanomaterials*, 2021, **11**(1), 212.

119 D. Yan, M. Meng, J. Li, J. Li and X. Li, Vanadium dioxide-assisted broadband absorption and linear-to-circular polarization conversion based on a single metasurface design for the terahertz wave, *Opt. Exp.*, 2020, **28**(20), 29843–29854.

120 Y. Qiu, D.-X. Yan, Q.-Y. Feng, X.-J. Li, L. Zhang and G.-H. Qiu, *et al.*, Vanadium dioxide-assisted switchable multifunctional metamaterial structure, *Opt. Exp.*, 2022, **30**(15), 26544–26556.

121 J. Xu, R. Yang, Y. Fan, Q. Fu and F. Zhang, A review of tunable electromagnetic metamaterials with anisotropic liquid crystals, *Front. Phys.*, 2021, **9**, 633104.

122 R. Wang, L. Li, J. Liu, F. Yan, F. Tian and H. Tian, *et al.*, Triple-band tunable perfect terahertz metamaterial absorber with liquid crystal, *Opt. Exp.*, 2017, **25**(26), 32280–32289.

123 O. M. Sanusi, Y. Wang and L. Roy, Reconfigurable polarization converter using liquid metal based metasurface, *IEEE Trans. Antennas Propag.*, 2021, **70**(4), 2801–2810.

124 D. Li, S. Yuan and R. Yang, Dynamical optical-controlled multi-state THz metamaterial absorber, *Acta Opt. Sin.*, 2020, **40**(8), 0816001.

125 S. Liao, J. Sui and H. Zhang, Switchable ultra-broadband absorption and polarization conversion metastructure controlled by light, *Opt. Exp.*, 2022, **30**(19), 34172–34187.

126 J. Li, J. Chen, D. Yan, F. Fan, K. Chen and K. Zhong, *et al.*, A review: Active tunable terahertz metamaterials, *Adv. Photon. Res.*, 2024, **5**(7), 2300351.

127 L. Li, T. Jun Cui, W. Ji, S. Liu, J. Ding and X. Wan, *et al.*, Electromagnetic reprogrammable coding-metasurface holograms, *Nat. Commun.*, 2017, **8**(1), 197.

128 X. Wan, M. Q. Qi, T. Y. Chen and T. J. Cui, Field-programmable beam reconfiguring based on digitally-controlled coding metasurface, *Sci. Rep.*, 2016, **6**(1), 20663.

129 X. G. Zhang, W. X. Jiang, H. L. Jiang, Q. Wang, H. W. Tian and L. Bai, *et al.*, An optically driven digital metasurface for programming electromagnetic functions, *Nat. Electron.*, 2020, **3**(3), 165–171.

130 Z. Wu, Y. Ra'di and A. Grbic, Tunable metasurfaces: A polarization rotator design, *Phys. Rev. X*, 2019, **9**(1), 011036.

131 L. Zeng, H.-F. Zhang and D. Zhang, A tunable metamaterial-based linear-to-circular polarization converter regulated solid state plasma in S-band, *J. Opt.*, 2020, **22**(12), 125103.

132 Y.-P. Li, H.-F. Zhang, T. Yang, T.-Y. Sun and L. Zeng, A multifunctional polarization converter base on the solid-state plasma metasurface, *IEEE J. Quantum Electron.*, 2020, **56**(2), 1–7.

133 R. Phon, S. Ghosh and S. Lim, Novel multifunctional reconfigurable active frequency selective surface, *IEEE Trans. Antennas Propag.*, 2018, **67**(3), 1709–1718.

134 H.-F. Zhang, X.-L. Tian, G.-B. Liu and X.-R. Kong, A gravity tailored broadband metamaterial absorber containing liquid dielectrics, *IEEE Access*, 2019, **7**, 25827–25835.

135 L. Zeng, H.-F. Zhang, G.-B. Liu and T. Huang, A three-dimensional Linear-to-Circular polarization converter tailored by the gravity field, *Plasmonics*, 2019, **14**(6), 1347–1355.

136 P. Min, Z. Song, L. Yang, V. G. Ralchenko and J. Zhu, Optically transparent flexible broadband metamaterial absorber based on topology optimization design, *Micromachines*, 2021, **12**(11), 1419.

137 D. Zong, L. Zhu, Z. Yu, Y. Liu, Y. Li and Y. Wang, Design of embedded metamaterial solar absorber based on genetic algorithm, *Results Phys.*, 2023, **50**, 106559.

138 J. Wang, W.-Q. Gu, X.-C. Zhao, Y.-N. Jiang and K.-D. Xu, Designing broadband cross-polarization conversion metasurfaces using binary particle swarm optimization algorithm, *Mater. Des.*, 2024, **247**, 113419.

139 J. Chen, W. Ding, X.-M. Li, X. Xi, K.-P. Ye and H.-B. Wu, *et al.*, Absorption and diffusion enabled ultrathin broadband metamaterial absorber designed by deep neural network and PSO, *IEEE Antennas Wirel. Propag. Lett.*, 2021, **20**(10), 1993–1997.

140 J. Gao, C. Feng, X. Wu, Y. Wu, X. Zhu and D. Sun, *et al.*, Deep neural network training method based on vector-graphs for designing of metamaterial broadband polarization converters, *Sci. Rep.*, 2023, **13**(1), 5009.

141 Y. Xiao, K. Chen and Y. Feng, Deep-learning-assisted Design of Polarization Conversion Metasurface with On-demand Frequency Response and Ultra-broadband Electromagnetic Scattering Reduction, IEEE Journal on Multiscale and Multiphysics Computational, *Techniques*, 2024, **9**, 258–266.

142 A. Shahsavaripour, M. H. Badiei, A. Kalhor and L. Yousefi, Design of thin, wideband electromagnetic absorbers with polarization and angle insensitivity using deep learning, *Sci. Rep.*, 2025, **15**(1), 9426.

143 Y. Jia, Y. Liu, W. Zhang and S. Gong, Ultra-wideband and high-efficiency polarization rotator based on metasurface, *Appl. Phys. Lett.*, 2016, **109**, 5.

144 X. Zhang, H. Ye, Y. Zhao and H. Zhang, A tunable ultra-wideband cross-polarization conversion based on the band splicing technology, *Appl. Phys. B*, 2021, **127**(5), 69.

145 T. M. Kollatou, A. I. Dimitriadis, S. Assimonis, N. V. Kantartzis and C. S. Antonopoulos, A family of ultra-thin, polarization-insensitive, multi-band, highly absorbing metamaterial structures, *Prog. Electromagn. Res.*, 2013, **136**, 579–594.

146 Z. Zhu, H. Wang, Y. Li, Y. Meng, W. Wang and L. Zheng, *et al.*, Origami-based metamaterials for dynamic control of wide-angle absorption in a reconfigurable manner, *IEEE Trans. Antennas Propag.*, 2022, **70**(6), 4558–4568.

147 Y.-Q. Bao, B.-X. Li and H.-F. Zhang, Tunable origami metastructure based on liquid crystal for curvature sensing, *Opt. Express*, 2024, **32**(4), 6432–6445.

148 L. Wang, Y. Wang, D. Liu, Y. Wang, X. Zhang and G. Wen, *et al.*, Carbon-Coated Octahedral Fe3O4/Fe2O3 Nanocomposites for Enhanced Electromagnetic Wave Absorption, *ACS Appl. Nano Mater.*, 2025, **8**(6), 2952–2964.

149 Y. Li, L. Zeng and H. Zhang, Technique for improving polarization conversion performance, *J. Opt. Soc. Am. B*, 2022, **39**(10), 2573–2581.

150 A. Gevorgyan, Reflection and transmission of light in medium/cholesteric/substrate and glass (1)/cholesteric/glass (2) systems, *Tech. Phys.*, 2000, **45**(9), 1170–1176.

151 S. Li, L.-R. Huang, Y.-H. Ling, W.-B. Liu, C.-F. Ba and H.-H. Li, High-performance asymmetric optical transmission based on coupled complementary subwavelength gratings, *Sci. Rep.*, 2019, **9**(1), 17117.

152 L. Lei, B.-F. Wan, S.-Y. Liao and H.-F. Zhang, Broadband asymmetric absorption-transmission and double-band rasorber of electromagnetic waves based on superconductor ceramics metastructures-photonic crystals, *Eng. Sci. Technol.*, 2024, **57**, 101810.

153 L. Lei, B.-F. Wan, S.-Y. Liao and H.-F. Zhang, Dual-channel asymmetric absorption-transmission properties based on plasma metastructures-photonic crystals, *Opt. Express*, 2024, **32**(22), 38023–38038.

154 D.-D. Zhu, Y. Lv, Y.-J. Yin and H.-F. Zhang, Broadband electromagnetic induction transparent and absorptive dual-function metastructure with vanadium dioxide doping, *Opt. Laser Technol.*, 2024, **179**, 111410.

155 J.-R. Wang and H.-F. Zhang, Multiple Physical Quantity Sensing and Logical Operation Realized by Electromagnetically Induced Absorption, *IEEE Trans. Instrum. Meas.*, 2025, **74**, 1–9.

156 Z.-H. Xing, S.-Y. Liao, Y. Zheng, X.-Z. Tang and H.-F. Zhang, Terahertz dual-mechanism dual-band linear-to-circular polarization converter with one-octave band separation and orthogonal polarization, *Opt. Exp.*, 2025, **33**(7), 14777–14795.

157 Z.-H. Xing, Q.-J. Li, S. Xu, S.-Y. Liao and H.-F. Zhang, Frequency-reconfigurable polarization conversion technology with one-octave band separation and consistent chirality, *Phys. Fluids*, 2025, **37**, 4.

158 W.-H. Jiao, Y.-M. Chang, L. Wang and W.-J. Wu, A dual-polarized frequency selective rasorber with wide transmission band, *Radio Sci.*, 2021, **56**(7), 1–12.

159 A. Kumar, G. Sen and J. Ghosh, Design of a Compact SRR Loaded Polarization-Independent Wideband Metamaterial Rasorber with a Narrow Transmission Window, *Prog. Electromagn. Res.*, 2025, **131**.

160 C. Yang, Y.-X. Wei, H.-J. Liu, X. Li and H.-F. Zhang, Design of a nonlinear metastructure for temperature detection and biosensing based on the second harmonic generation in theory, *J. Mater. Chem. B*, 2025, **29**, 8573–8942.

161 T.-S. Yao, J.-Y. Sui, R. Du, T.-H. Zhang and H.-F. Zhang, A layered metastructure-based smart radiant regulator with enhanced emissivity modulation utilizing phase change material, *Int. Commun. Heat Mass Transfer*, 2025, **164**, 108933.

162 S. Dai, Y.-Q. Bao, J.-R. Pan and H.-F. Zhang, A frequency-reconfigurable conformal metastructure absorber with liquid crystal temperature control for RCS reduction, *J. Mater. Chem. C*, 2025, **24**, 12031–12568.

163 J.-H. Zou, J.-Y. Sui and H.-F. Zhang, A logic metastructure for register function implementation, *Appl. Phys. Lett.*, 2025, **126**, 21.

This journal is © the Owner Societies 2025

Phys. Chem. Chem. Phys., 2025, **27**, 25720–25742 | 25741

164 X. Jiang, H. Yuan, X. He, T. Du, H. Ma and X. Li, *et al.*, Implementing of infrared camouflage with thermal management based on inverse design and hierarchical metamaterial, *Nanophotonics*, 2023, **12**(10), 1891–1902.

165 S. Wu, H. Huang, Z. Huang, C. Tian, L. Guo and Y. Liu, *et al.*, Multifunctional Hierarchical Metamaterials: Synergizing Visible-Laser-Infrared Camouflage with Thermal Management, *Photonics*, 2025, **12**(4), 387.